

Electronic Supplementary Information for

Tetraphenylethylene-based photoresponse supramolecular organic framework and its metallization for photocatalytic redox reactions

Fa-Dong Wang,^{a†} Kai-Kai Niu,^{a†} Xian-Ya Yao,^a Shengsheng Yu,^a Hui Liu,^a Ling-Bao Xing*^a and Pei-Zhou Li*^b

^aSchool of Chemistry and Chemical Engineering, Shandong University of Technology, Zibo 255000, P. R. China

^bSchool of Chemistry and Chemical Engineering, Shandong Provincial Key Laboratory for Science of Material Creation and Energy Conversion, Science Center for Material Creation and Energy Conversion, Shandong University, Ji'nan 250100, P. R. China

[†]These authors contributed equally to this work.

E-mail: lbxing@sdu.edu.cn; pzli@sdu.edu.cn.

1. Experimental section

Materials

Unless specifically mentioned, all chemicals are commercially available and were used as received.

Characterization

¹H NMR spectra was recorded on a Bruker Advance 400 spectrometer (400 MHz) at 298 K, and the chemical shifts (δ) were expressed in ppm and J values were given in Hz. UV-vis spectra were obtained on a Shimadzu UV-1601PC spectrophotometer in a quartz cell (light path 10 mm) at 298 K. Steady-state fluorescence measurements were carried out using a Hitachi 4500 spectrophotometer. Dynamic light scattering (DLS) and zeta potential are measured on Malvern Zetasizer Nano ZS90. Transmission electron microscopy (TEM) images were obtained on a JEM 2100 operating at 120 kV. Samples for TEM measurements were prepared by dropping the mixture aqueous solution on carbon-coated copper grid (300 mesh) and drying by slow evaporation. Inductively coupled plasma-mass spectrometry (ICP-MS) data were obtained with an Agilent 7800x ICP-MS and analyzed using ICP-MS Mass Hunter. The photocatalytic reaction was performed on WATTCAS Parallel Photocatalytic Reactor (WP-TEC-HSL) with 10W COB LED.

Detection of $^1\text{O}_2$ production in solution

Compound 9,10-anthracenediyl-bis(methylene)-dimalonic acid (ABDA) was used as an indicator for detection of $^1\text{O}_2$ in solution (Fig. S6). 50 μM of photocatalyst was dissolved in 3.0 mL solution containing 250 μM of ABDA. The mixture was then placed in a cuvette and irradiated with a UV LEDs (365-367 nm). The absorption change of the sample at 378 nm was recorded by the UV-Vis absorption spectrophotometer.

Detection of $\text{O}_2^\cdot-$ production in solution

N,N,N',N'-tetramethyl-phenylenediamine (TMPD) was used as the scavenger monitors $\text{O}_2^\cdot-$. The 5 mM TMPD solution in DMSO was added to the aqueous solution to form a 0.25 mM solution. 50 μM NA-TPE, 50 μM MV-DPY and 50 μM MVDPY-NATPE-CB[8] were added into TMPD solution respectively for $\text{O}_2^\cdot-$ generation measurement. The mixture was then placed in a cuvette and irradiated with UV LEDs (365-367 nm). The generation of $\text{O}_2^\cdot-$ was detected by monitoring the absorption at 612 nm through UV-vis absorption spectra.

General procedure for the aerobic oxidation reaction of *N*-phenyltetrahydroisoquinoline

N-phenyltetrahydroisoquinoline (0.1 mmol, 20.9 mg) was added in the newly produced solution of MVDPY-NATPE-CB[8] (1.0 mol%, 3.0 mL, [NA-TPE] = 3.33×10^{-4} M, [MV-DPY] = 6.67×10^{-4} M, CB[8] = 1.33×10^{-3} M). The reaction was irradiated with UV LEDs (10 W, 365 nm-367 nm) at room temperature under the ambient air condition for 24 h. Then the mixture was extracted with dichloromethane, and the combined organic layer was dried with anhydrous Na_2SO_4 . Then the organic solvent was removed in vacuo and purified by flash column chromatography with petroleum ether/ethyl acetate to afford the products.

General procedure for the aerobic oxidation reaction of 1,2-diphenylhydrazine

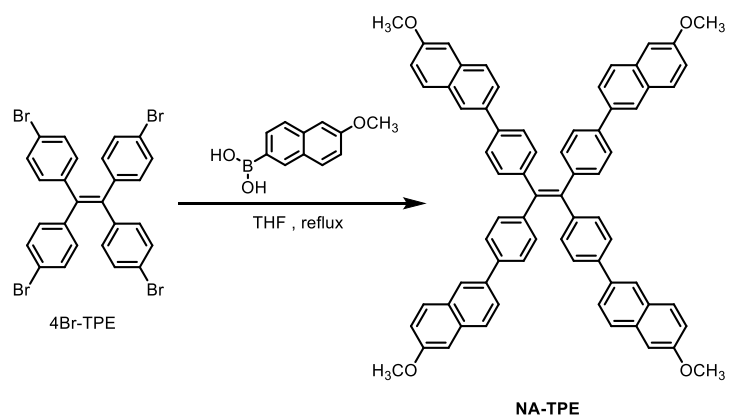
1,2-Diphenylhydrazine (0.2 mmol, 36.4 mg) was added in the newly produced solution of MVDPY-NATPE-CB[8] (1.0 mol%, 3.0 mL, [NA-TPE] = 3.33×10^{-4} M,

$[MV-DPY] = 6.67 \times 10^{-4}$ M, $[CB[8]] = 1.33 \times 10^{-3}$ M). The reaction was irradiated with UV LEDs (10 W, 365 nm-367 nm) at room temperature under the ambient air condition for 24 h. Then the mixture was extracted with dichloromethane, and the combined organic layer was dried with anhydrous Na_2SO_4 . Then the organic solvent was removed in vacuo and purified by flash column chromatography with petroleum ether/ethyl acetate to afford the products.

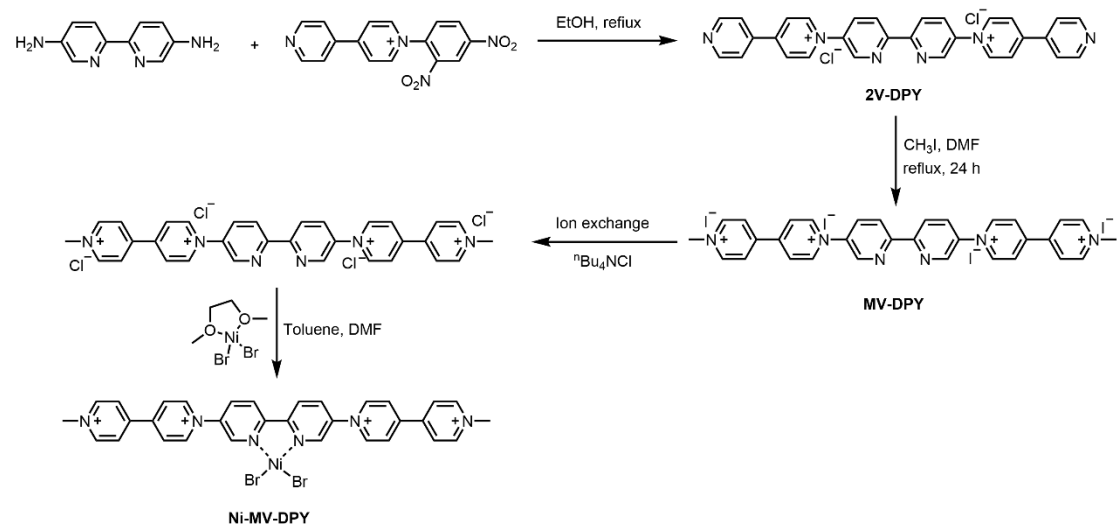
General procedure for the photocatalytic cross coupling reaction of p-toluenesulphenol and 4'-bromoacetophenone

4'-Bromoacetophenone (0.2 mmol, 39.8 mg), p-toluenesulphenol (0.2 mmol, 49.8 mg) was added in the newly produced solution of Ni- MVDPY-NATPE-CB[8] (1.0 mol%, 3.0 mL, $[NA-TPE] = 3.33 \times 10^{-4}$ M, $[Ni-MV-DPY] = 6.67 \times 10^{-4}$ M, $[CB[8]] = 1.33 \times 10^{-3}$ M). The reaction was irradiated with UV LEDs (10 W, 365 nm-367 nm) at room temperature under the ambient air condition for 24 h. Then the mixture was extracted with dichloromethane, and the combined organic layer was dried with anhydrous Na_2SO_4 . Then the organic solvent was removed in vacuo and purified by flash column chromatography with petroleum ether/ethyl acetate to afford the products.

Synthesis of NA-TPE and Ni-MV-DPY



Scheme S1 Synthetic route of NA-TPE.



Scheme S2 Synthetic route of MV-DPY and Ni-MV-DPY.

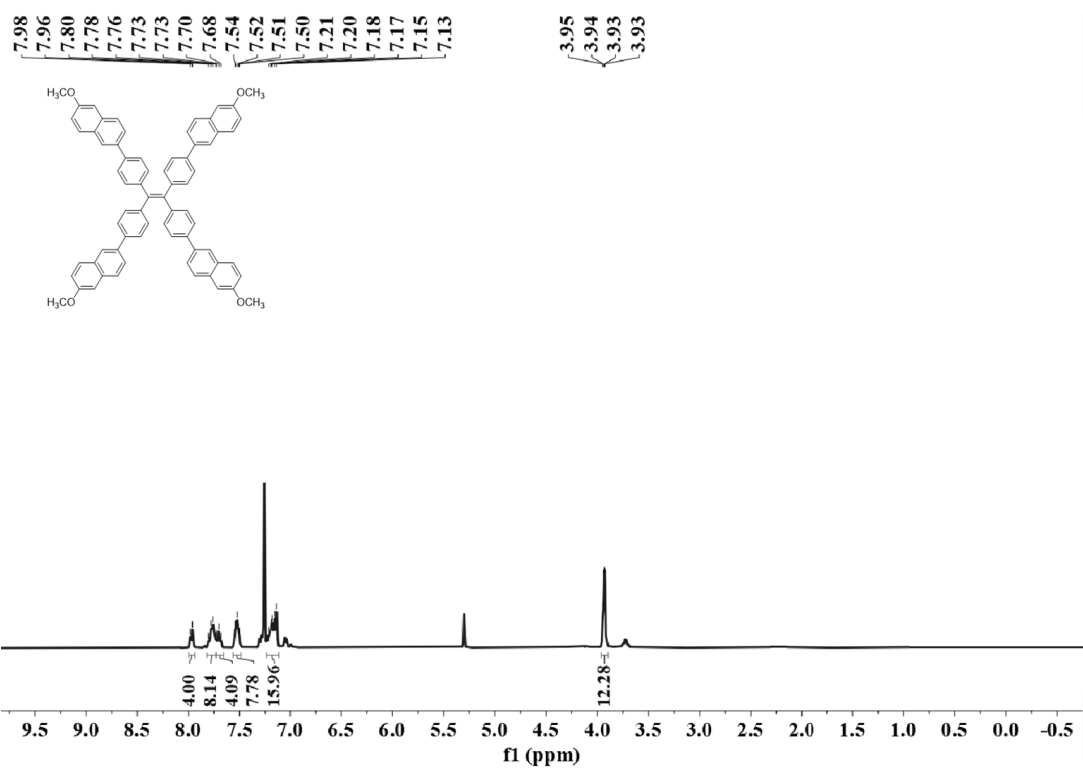


Fig. S1 ^1H NMR spectrum of compound NA-TPE in CDCl_3 .

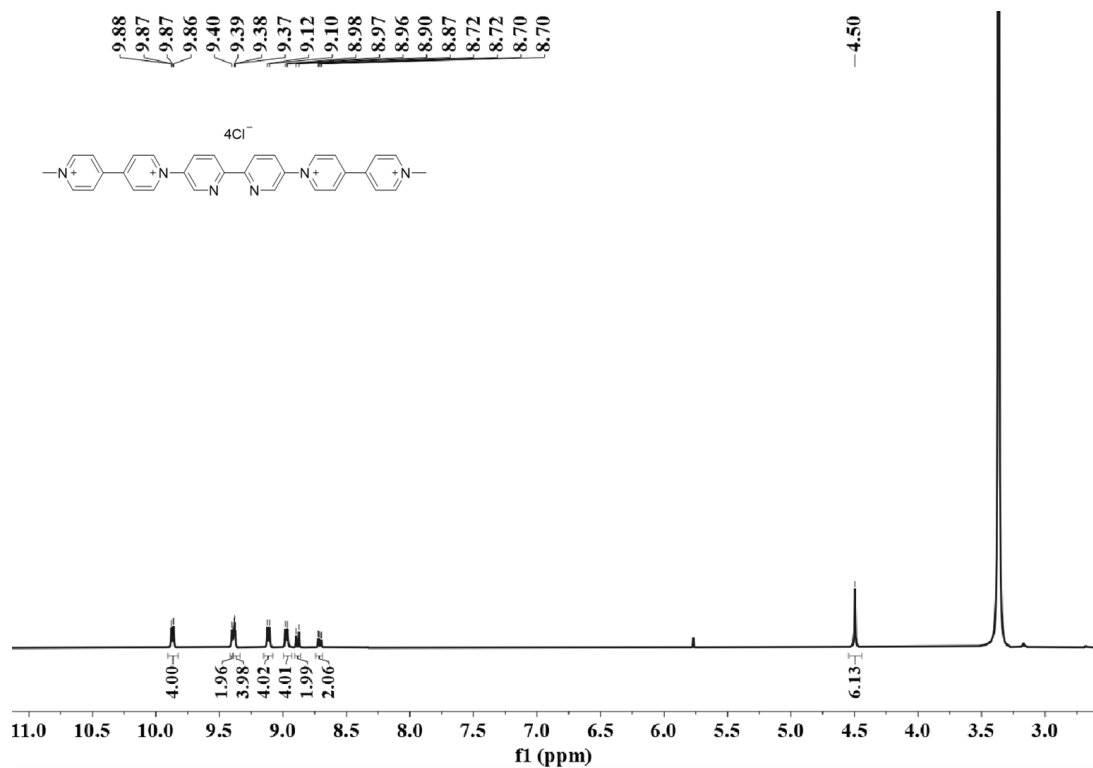


Fig. S2 ^1H NMR spectrum of compound MV-DPY in $\text{DMSO}-d_6$.

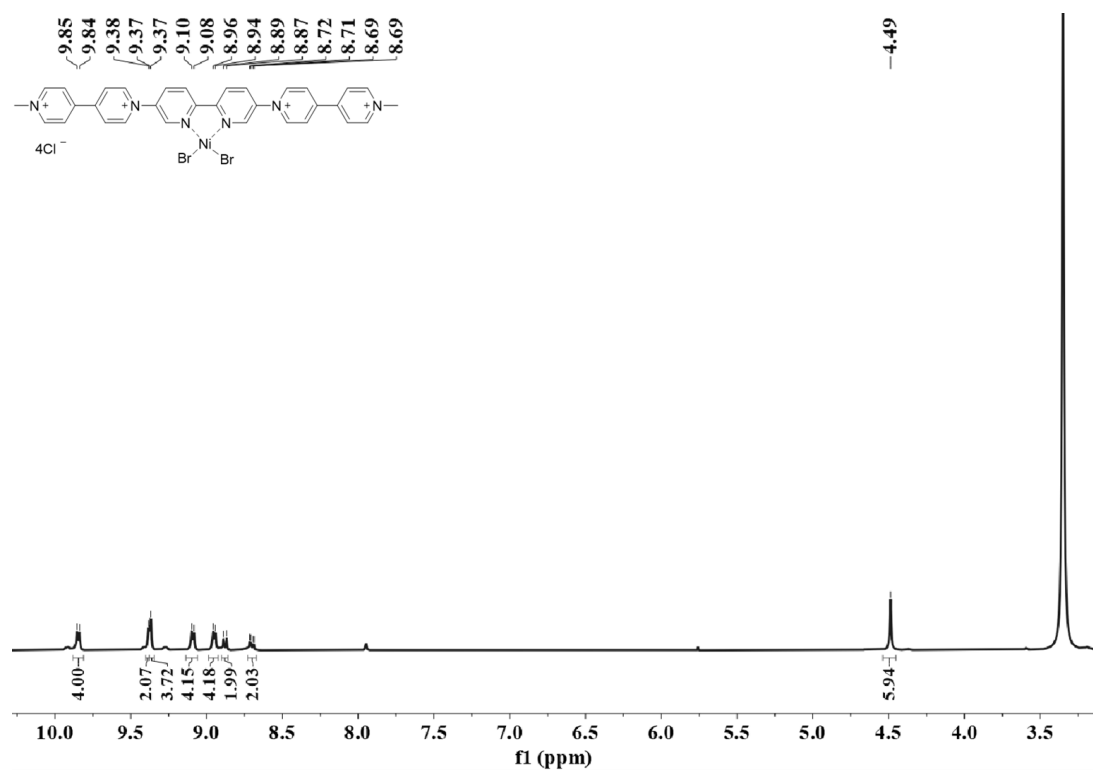


Fig. S3 ^1H NMR spectrum of compound Ni-MV-DPY in $\text{DMSO}-d_6$.

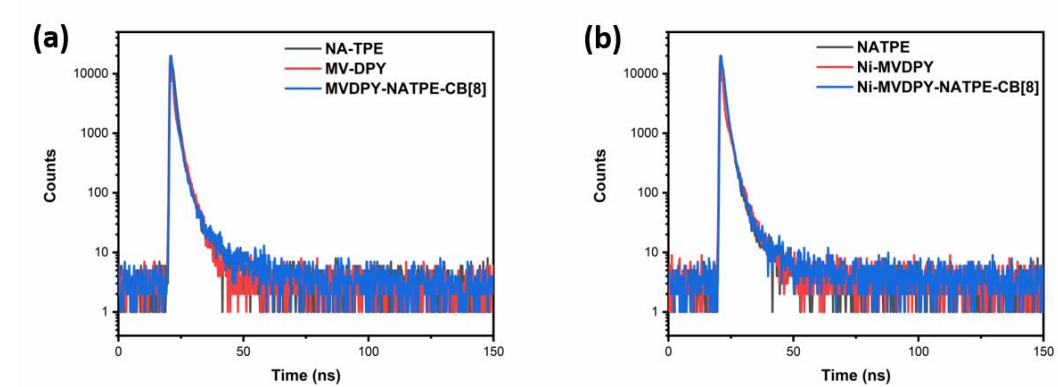


Fig. S4 Time-resolved fluorescence decay curves of (a) NA-TPE, MV-DPY, and MVDPY-NATPE-CB[8] and (b) NA-TPE, Ni-MV-DPY, and Ni-MVDPY-NATPE-CB[8].

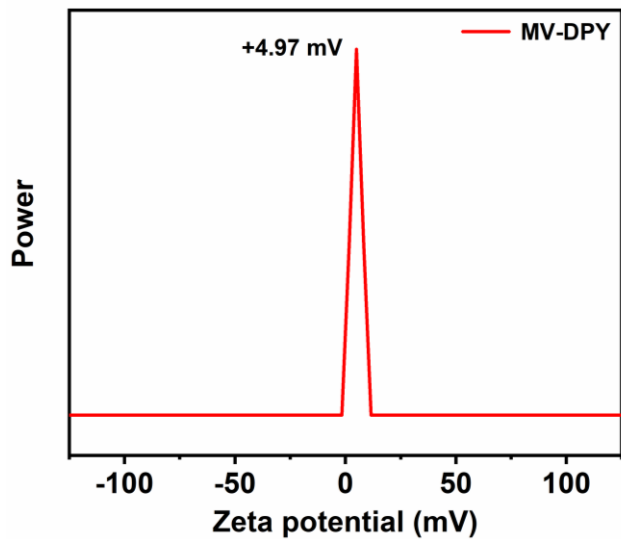


Fig. S5 Zeta potential of MV-DPY (2.0×10^{-5} M).

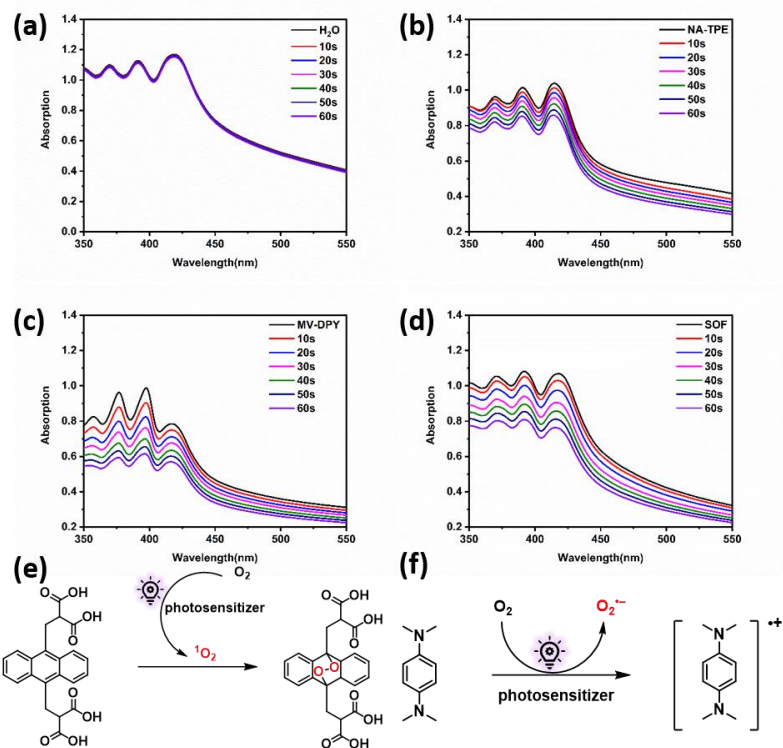


Fig. S6 UV-vis absorption spectra of (a) ABDA + H₂O, (b) ABDA + NA-TPE (5.0×10^{-5} M, 1.0×10^{-5} M), (c) ABDA + MV-DPY (5.0×10^{-5} M, 2.0×10^{-5} M) and (d) ABDA + SOF (5.0×10^{-5} M, 1.0×10^{-5} M) after irradiated by UV LEDs for different times; The reaction mechanism of (e) ABDA with $^1\text{O}_2$ and (f) TMPD with $\text{O}_2^{\cdot-}$.

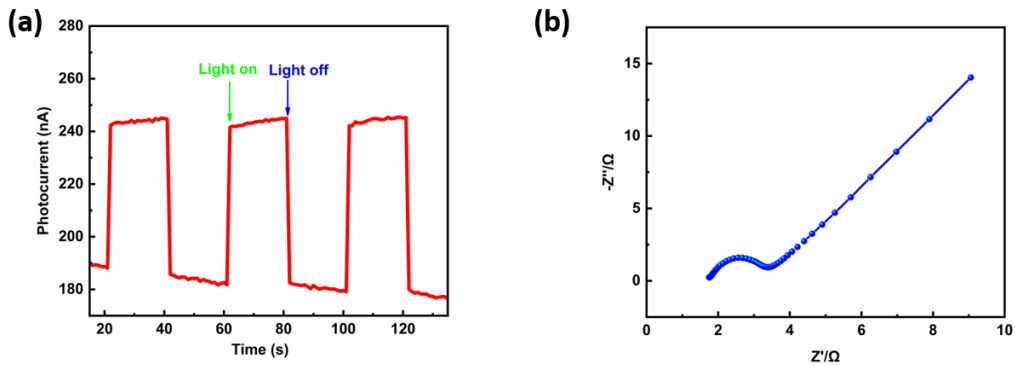


Fig. S7 (a) The transient photocurrent response and (b) The electrochemical impedance spectra of MVDPY-NATPE-CB[8].

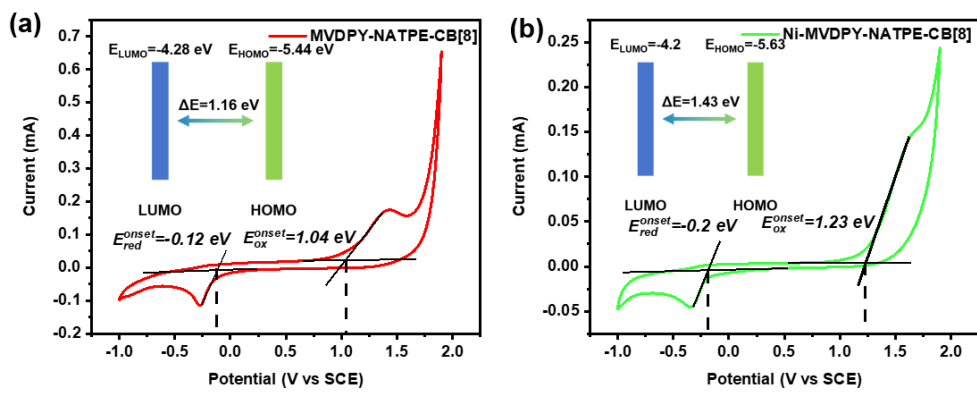


Fig. S8 Cyclic voltammograms of (a) MVDPY-NATPE-CB[8] and (b) Ni-MVDPY-NATPE-CB[8].

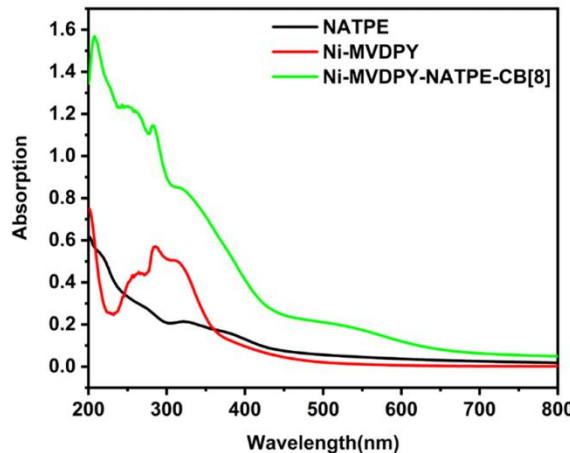
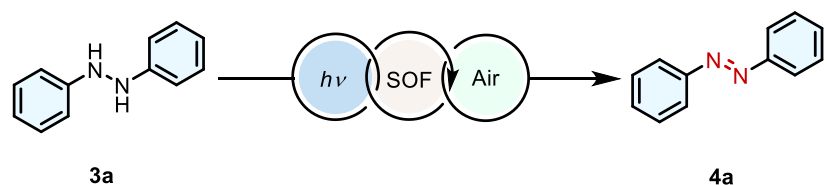


Fig. S9 UV-vis absorption spectra of MV-DPY ($2.0 \times 10^{-5} \text{ M}$), Ni-MV-DPY ($2.0 \times 10^{-5} \text{ M}$) and Ni-MV-DPY-NATPE-CB[8] ($2.0 \times 10^{-5} \text{ M}$) in the aqueous solution.

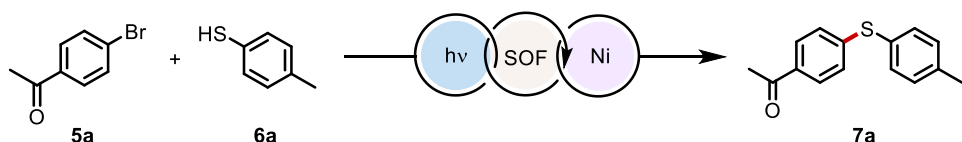
Table S1. Optimization of the aerobic oxidation reaction of 1,2-diphenylhydrazine conditions.^{a,b}



Entry	Variation from standard conditions	Yield ^b (%)
1	None	86
2	NA-TPE	No reaction
3	MV-DPY	33
4	0.5 mol% SOF	54
5	2.0 mol% SOF	88
6	18 h	64
7	32 h	87
8	No light	No reaction

^aReaction conditions: 1,2-diphenylhydrazine (0.2 mmol, 36.4 mg), DMVPY-NATPE-CB[8] as photocatalyst, UV LEDs (365-367 nm), room temperature, 24 h; ^bIsolated yield.

Table S2. Optimization of the cross coupling reaction of p-toluenesulphenol and 4'-bromoacetophenone conditions.^{c,d}

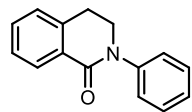


Entry	Variation from standard conditions	Yield ^b (%)
1	None	80
2	NA-TPE	No reaction
3	MV-DPY	25
4	0.5 mol% SOF-Ni	51
5	2.0 mol% SOF-Ni	82
6	18 h	56
7	32 h	81
8	No light	No reaction

^cStandard conditions: **1a** (0.20 mmol, 39.8 mg), **2a** (0.40 mmol, 24.9 mg), pyridine (0.2 mmol, 15.8 mg), 1.0 mol% Ni-DMVPY-NATPE-CB[8] as photocatalyst, UV LEDs (365-367 nm), room temperature, 24 h; ^dIsolated yield.

¹H NMR and ¹³C NMR data of 2a-2f, 4a-4i, and 7a-7f

2a. 2-phenyl-3,4-dihydroisoquinolin-1(2H)-one



83% yield; ¹H NMR (400 MHz, CDCl₃) δ 8.15 (d, J = 7.7 Hz, 1H), 7.46 (t, J = 7.4 Hz, 1H), 7.37 (t, J = 7.6 Hz, 1H), 7.24 (q, J = 8.3 Hz, 6H), 3.97 (t, J = 6.4 Hz, 2H), 3.14 (t, J = 6.5 Hz, 2H).

¹³C NMR (101 MHz, CDCl₃) δ 164.25, 143.11, 138.32, 132.07, 129.73, 128.96, 128.78, 127.24, 126.97, 126.29, 125.34, 49.44, 28.65.

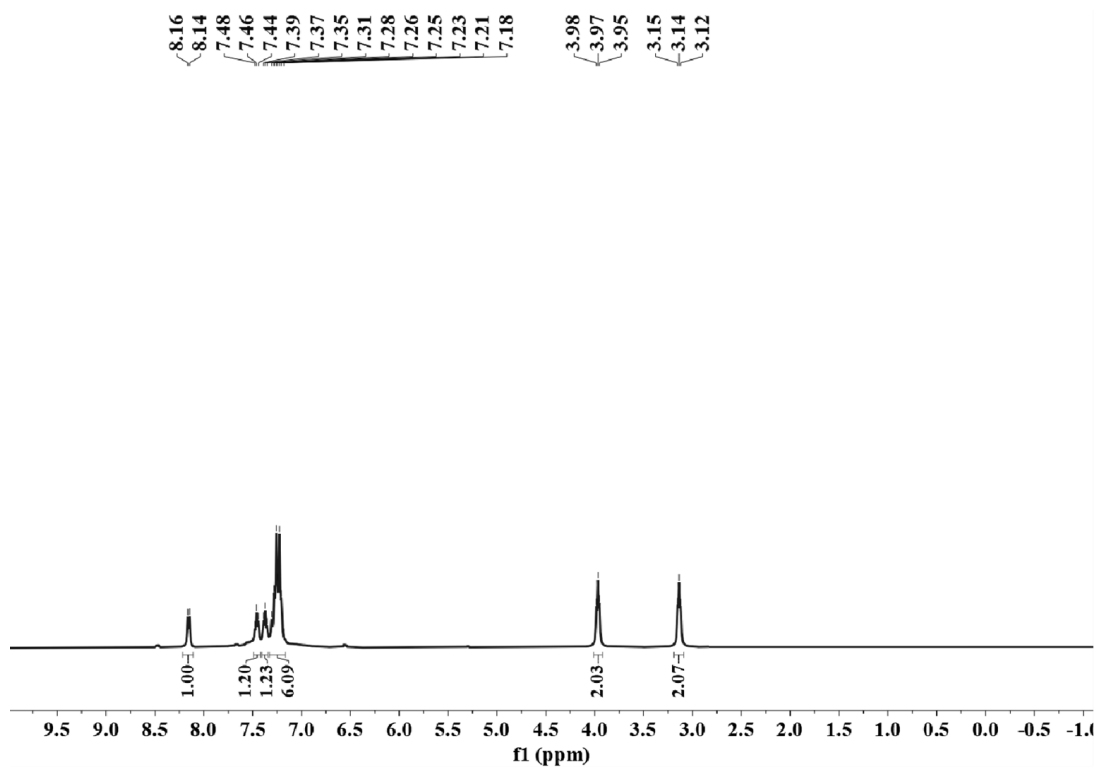


Fig. S10 ¹H NMR spectra of 2-phenyl-3,4-dihydroisoquinolin-1(2H)-one in CDCl₃.

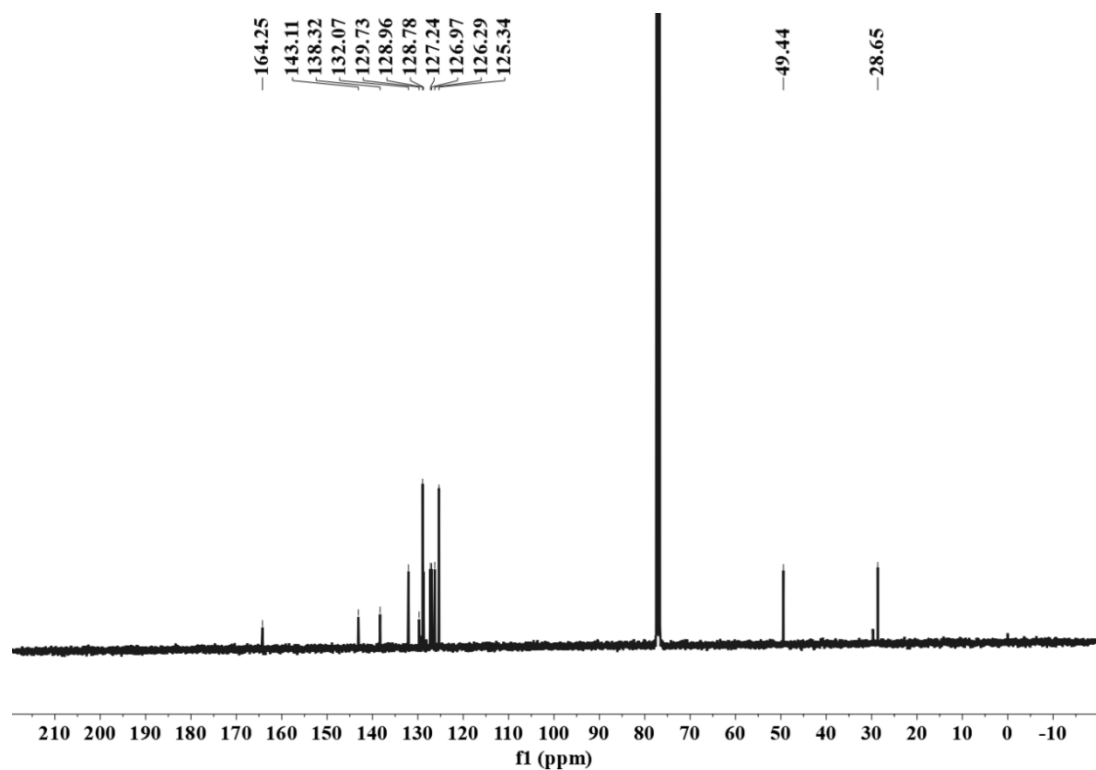
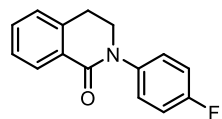


Fig. S11 ^{13}C NMR spectra of 2-phenyl-3,4-dihydroisoquinolin-1(2H)-one in CDCl_3 .

2b. 2-(4-fluorophenyl)-3,4-dihydroisoquinolin-1(2H)-one



86% yield; ^1H NMR (400 MHz, CDCl_3) δ 8.15 (dd, J = 7.7, 1.5 Hz, 1H), 7.48 (td, J = 7.5, 1.5 Hz, 1H), 7.42 - 7.32 (m, 3H), 7.25 (d, J = 8.2 Hz, 1H), 7.14 - 7.07 (m, 2H), 3.97 (dd, J = 7.0, 6.0 Hz, 2H), 3.16 (t, J = 6.4 Hz, 2H).

^{13}C NMR (101 MHz, CDCl_3) δ 164.40, 139.07, 138.26, 132.19, 129.49, 128.75, 127.29, 127.16, 127.07, 127.03, 115.89, 115.67, 49.58, 28.60.

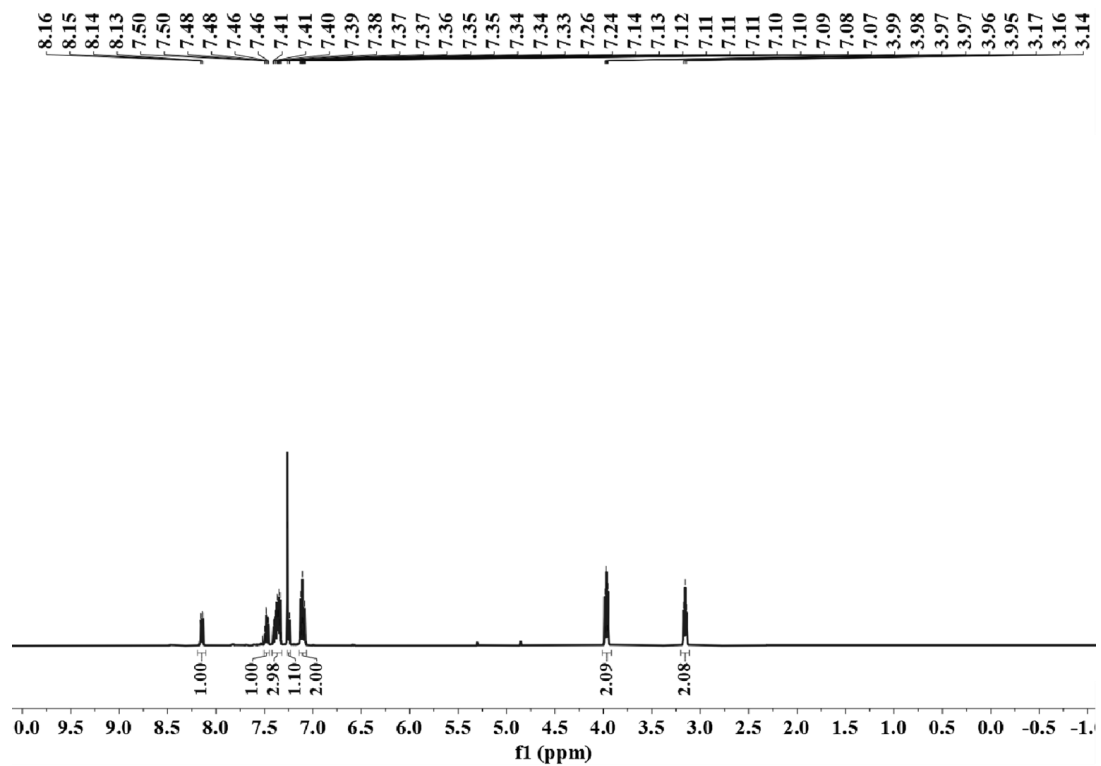


Fig. S12 ^1H NMR spectra of 2-(4-fluorophenyl)-3,4-dihydroisoquinolin-1(2H)-one in CDCl_3 .

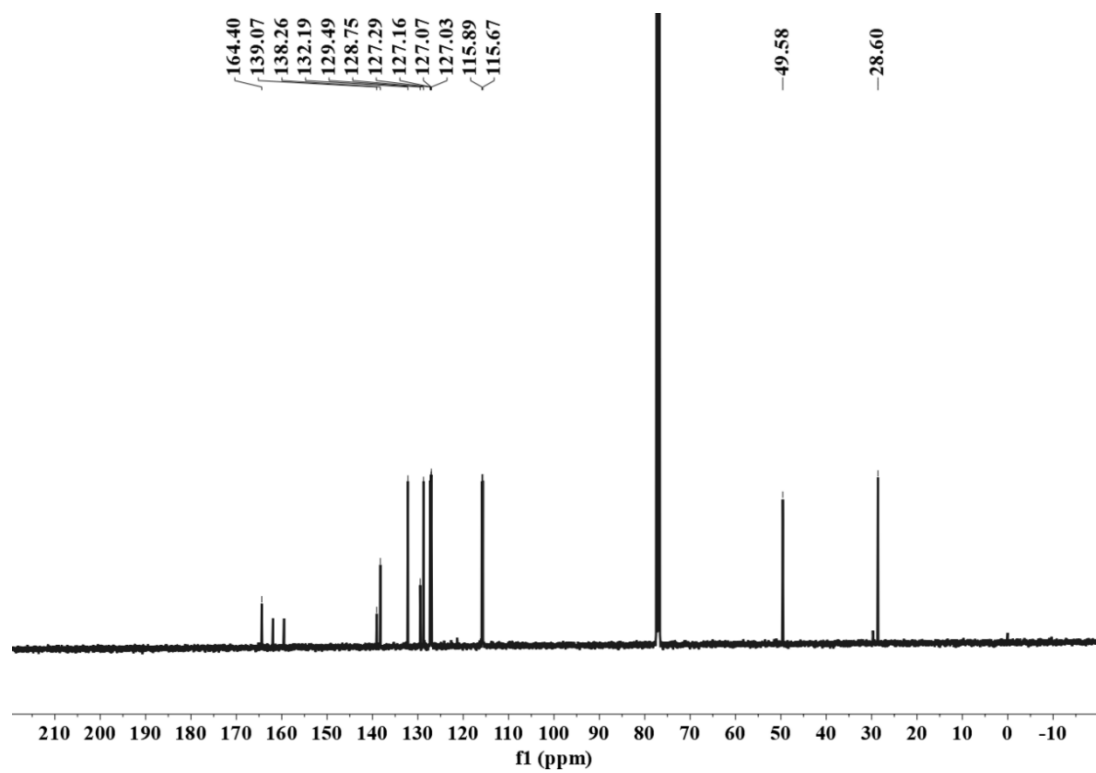
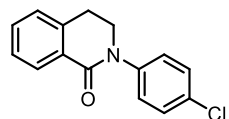


Fig. S13 ^{13}C NMR spectra of 2-(4-fluorophenyl)-3,4-dihydroisoquinolin-1(2H)-one in CDCl_3 .

2c. 2-(4-chlorophenyl)-3,4-dihydroisoquinolin-1(2H)-one



84% yield; ^1H NMR (400 MHz, CDCl_3) δ 8.07 (dd, J = 7.8, 1.5 Hz, 1H), 7.41 (td, J = 7.5, 1.5 Hz, 1H), 7.29 (dd, J = 15.6, 8.9, 6.4, 3.2 Hz, 5H), 7.20 - 7.16 (m, 1H), 3.90 (t, J = 6.5 Hz, 2H), 3.08 (t, J = 6.4 Hz, 2H).

^{13}C NMR (101 MHz, CDCl_3) δ 163.19, 140.50, 137.19, 131.22, 130.52, 128.36, 127.95, 127.73, 126.26, 125.99, 125.50, 48.27, 27.50.

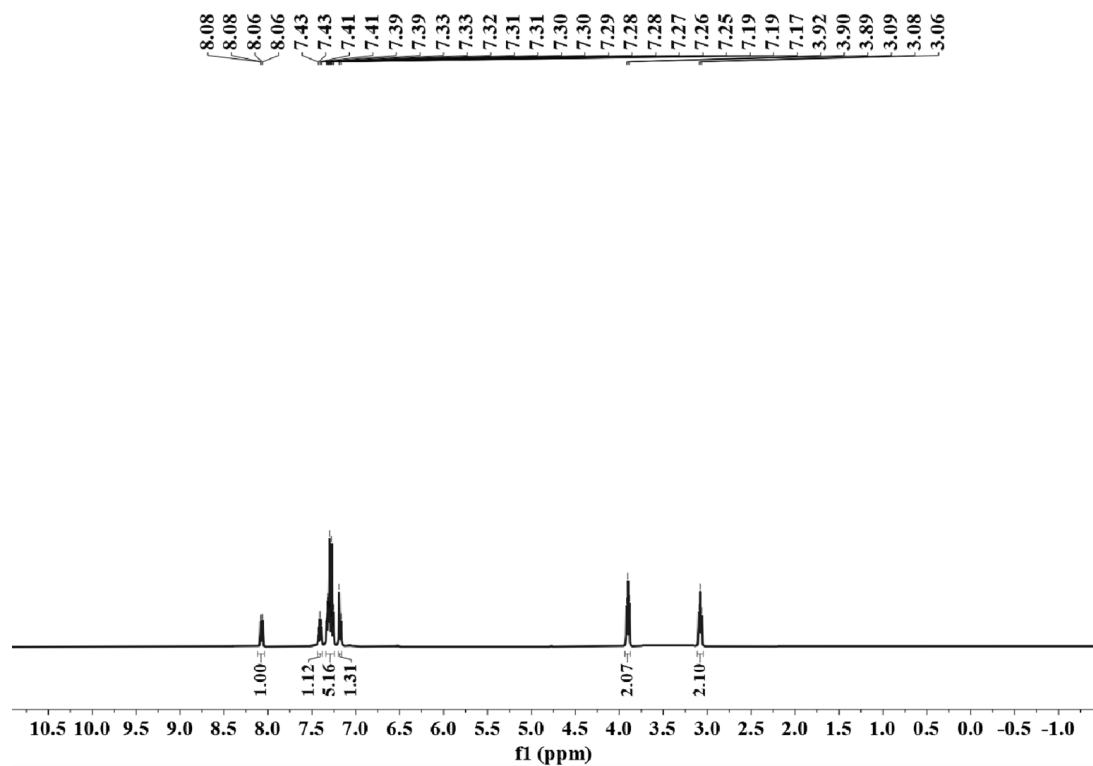


Fig. S14 ^1H NMR spectra of 2-(4-chlorophenyl)-3,4-dihydroisoquinolin-1(2H)-one in CDCl_3 .

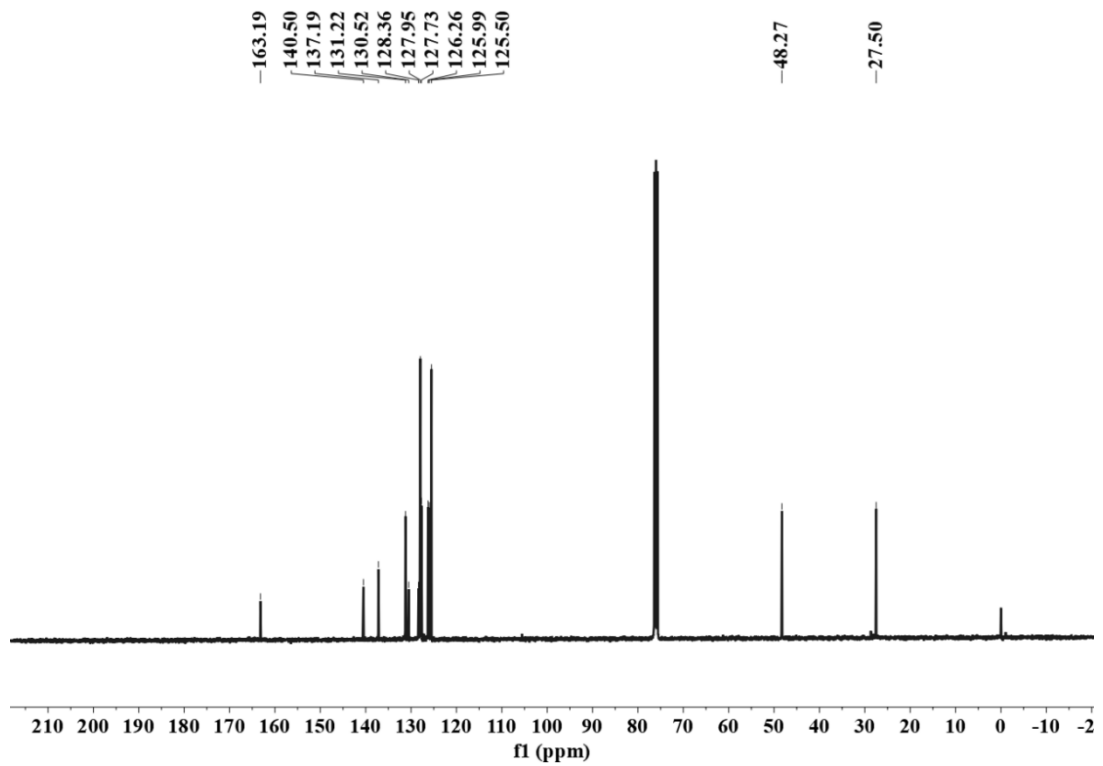
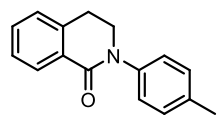


Fig. S15 ^{13}C NMR spectra of 2-(4-chlorophenyl)-3,4-dihydroisoquinolin-1(2H)-one in CDCl_3 .

2d. 2-(p-tolyl)-1,2,3,4-tetrahydroisoquinoline



80% yield; ^1H NMR (400 MHz, CDCl_3) δ 8.15 (dd, J = 7.8, 1.5 Hz, 1H), 7.46 (td, J = 7.5, 1.5 Hz, 1H), 7.37 (td, J = 7.6, 1.3 Hz, 1H), 7.29 (d, J = 10.7 Hz, 1H), 7.26 - 7.18 (m, 4H), 3.99 - 3.93 (m, 2H), 3.13 (t, J = 6.5 Hz, 2H), 2.36 (s, 3H).

^{13}C NMR (101 MHz, CDCl_3) δ 140.57, 138.31, 136.10, 131.97, 129.80, 129.58, 128.74, 127.19, 126.94, 125.23, 49.53, 28.66, 21.09.

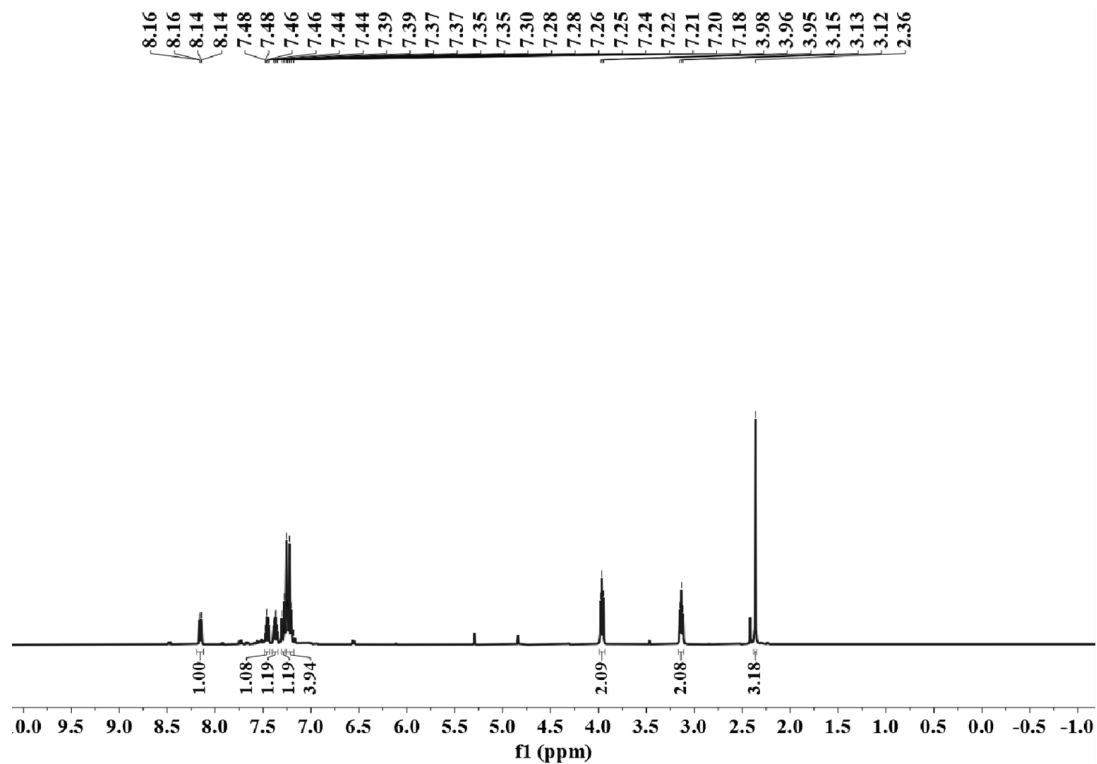


Fig. S16 ^1H NMR spectra of 2-(p-tolyl)-1,2,3,4-tetrahydroisoquinoline in CDCl_3 .

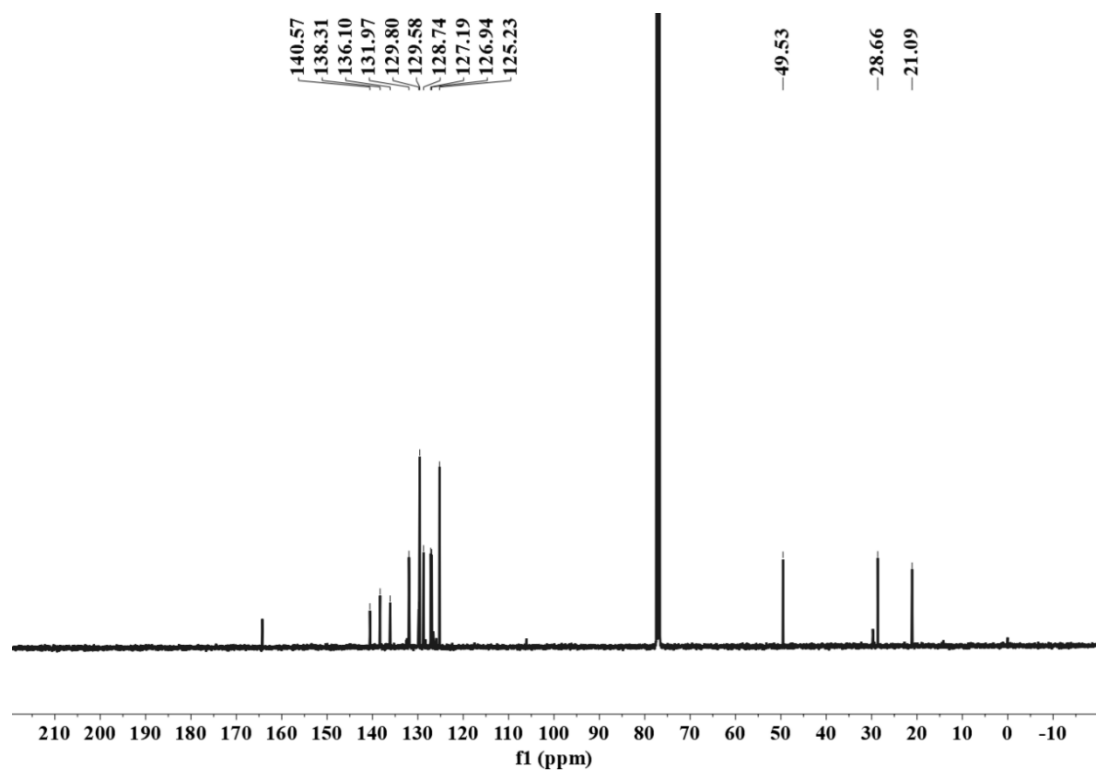
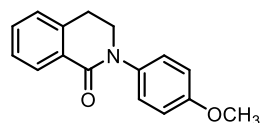


Fig. S17 ^{13}C NMR spectra of 2-(p-tolyl)-1,2,3,4-tetrahydroisoquinoline in CDCl_3 .

2e. 2-(4-methoxyphenyl)-3,4-dihydroisoquinolin-1(2H)-one



76% yield; ^1H NMR (400 MHz, CDCl_3) δ 8.15 (dd, $J = 7.7, 1.4$ Hz, 1H), 7.46 (td, $J = 7.5, 1.5$ Hz, 1H), 7.37 (td, $J = 7.5, 1.5$ Hz, 1H), 7.32 - 7.27 (m, 2H), 7.26 - 7.21 (m, 1H), 6.97 - 6.91 (m, 2H), 3.95 (dd, $J = 7.0, 6.0$ Hz, 2H), 3.83 (s, 3H), 3.14 (t, $J = 6.5$ Hz, 2H).

^{13}C NMR (101 MHz, CDCl_3) δ 164.44, 157.82, 138.30, 136.10, 131.96, 129.76, 128.71, 127.19, 126.95, 126.69, 114.26, 55.59, 55.53, 49.73, 28.66.

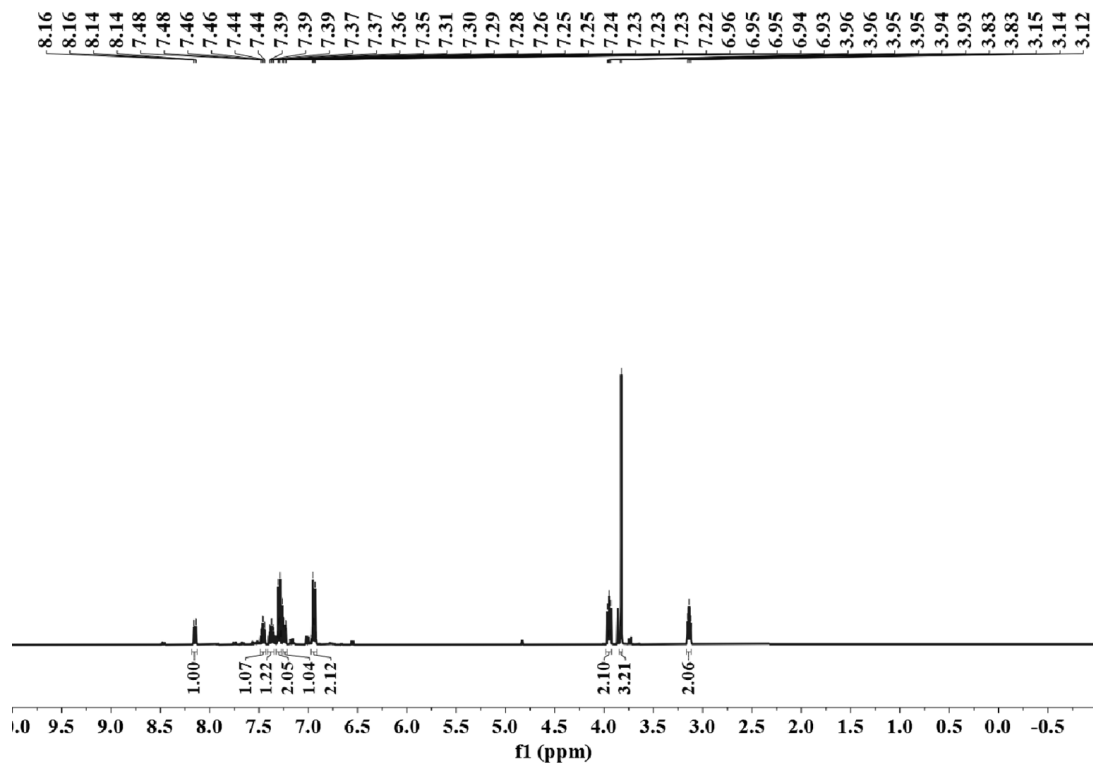


Fig. S18 ^1H NMR spectra of 2-(4-methoxyphenyl)-3,4-dihydroisoquinolin-1(2H)-one in CDCl_3 .

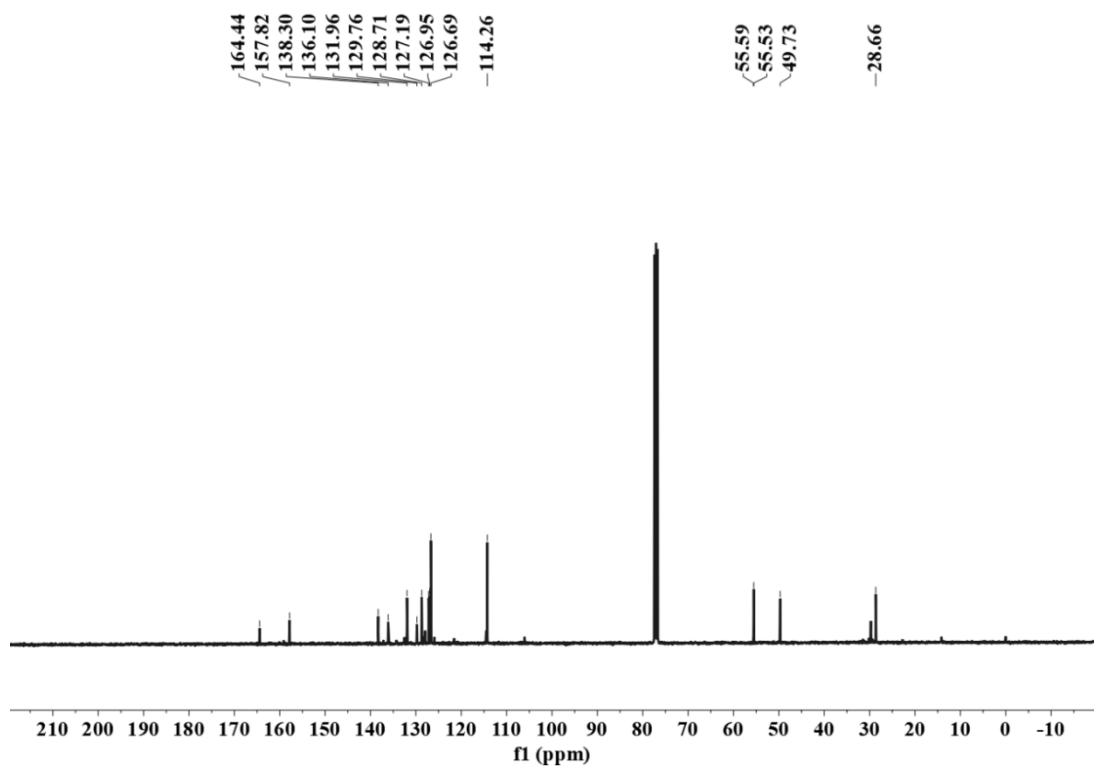
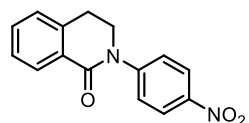


Fig. S19 ^{13}C NMR spectra of 2-(4-methoxyphenyl)-3,4-dihydroisoquinolin-1(2H)-one in CDCl_3 .

2f. 2-(p-nitrobenzene)-1,2,3,4-tetrahydroisoquinoline



87% yield; ^1H NMR (400 MHz, CDCl_3) δ 8.29 (d, J = 8.6 Hz, 1H), 8.17 (d, J = 7.8 Hz, 1H), 7.61 (d, J = 8.7 Hz, 1H), 7.51 (d, J = 7.5 Hz, 1H), 7.42 (t, J = 7.8 Hz, 1H), 7.28 (d, J = 11.6 Hz, 1H), 4.09 (t, J = 6.4 Hz, 1H), 3.20 (t, J = 6.4 Hz, 1H).

^{13}C NMR (101 MHz, CDCl_3) δ 164.22, 148.66, 144.74, 138.22, 132.83, 129.07, 128.94, 127.55, 127.16, 124.80, 124.30, 48.99, 29.73.

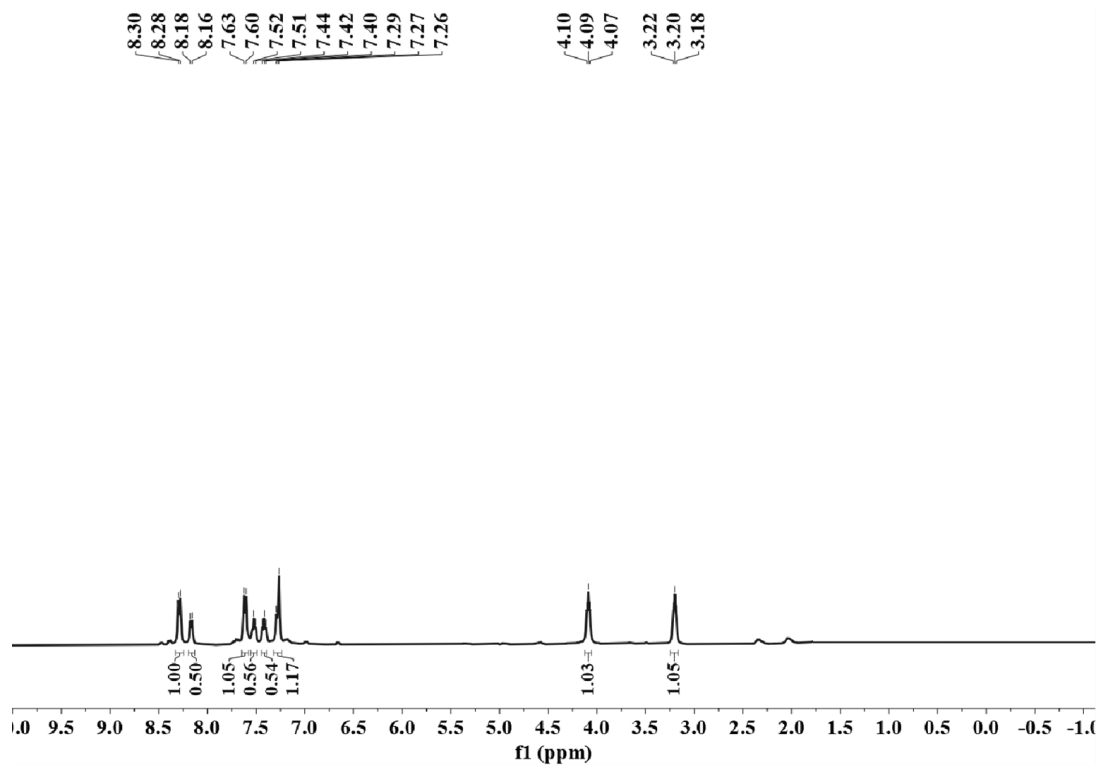


Fig. S20 ^1H NMR spectra of 2-(p-nitrobenzene) -1,2,3,4-tetrahydroisoquinoline in CDCl_3 .

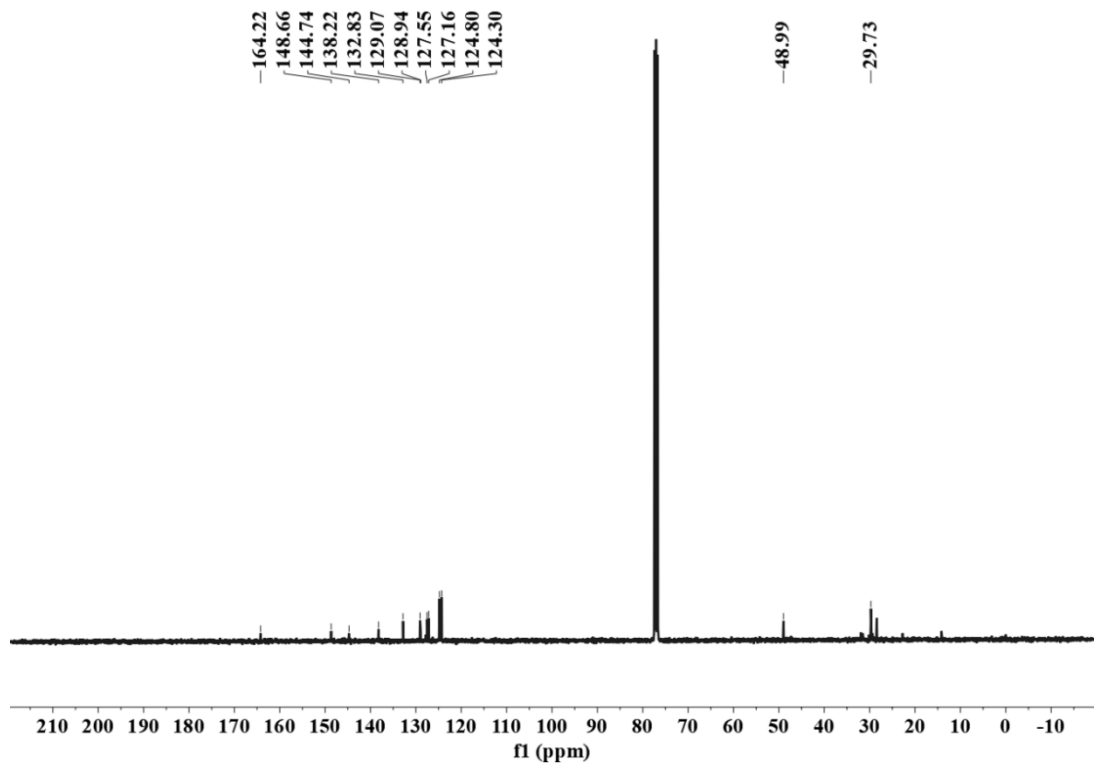
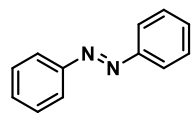


Fig. S21 ^{13}C NMR spectra of 2-(p-nitrobenzene)-1,2,3,4-tetrahydroisoquinoline in CDCl_3 .

4a. 1,2-diphenylhydrazine



86% yield; ^1H NMR (400 MHz, CDCl_3) δ 7.96 - 7.89 (m, 4H), 7.56 - 7.44 (m, 6H).

^{13}C NMR (101 MHz, CDCl_3) δ 152.61, 131.04, 129.12, 122.85.

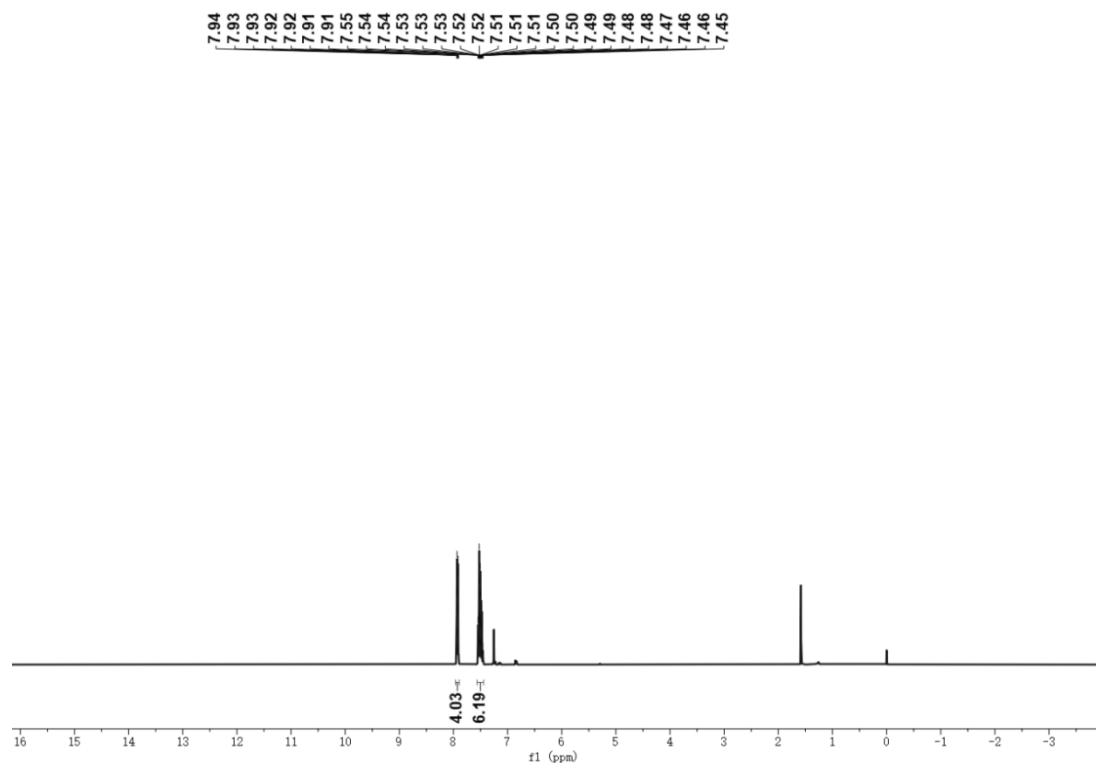


Fig. S22 ^1H NMR spectra of 1,2-diphenylhydrazine in CDCl_3 .

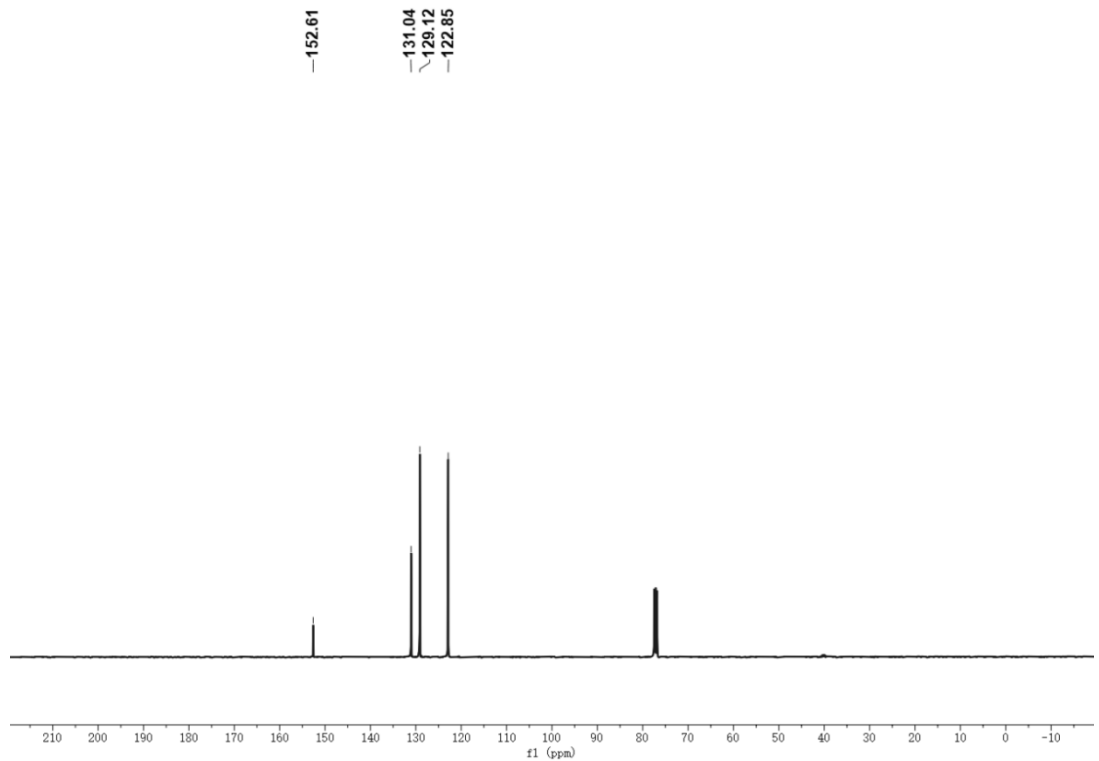
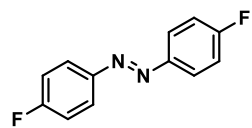


Fig. S23 ^{13}C NMR spectra of 1,2-diphenylhydrazine in CDCl_3 .

4b. 4,4'-difluoroazobenzene



93% yield; ^1H NMR (400 MHz, CDCl_3) δ 7.98 - 7.86 (m, 4H), 7.25 - 7.15 (m, 4H).

^{13}C NMR (101 MHz, CDCl_3) δ 165.62, 163.12, 148.97, 148.94, 124.87, 124.78, 116.21, 115.98.

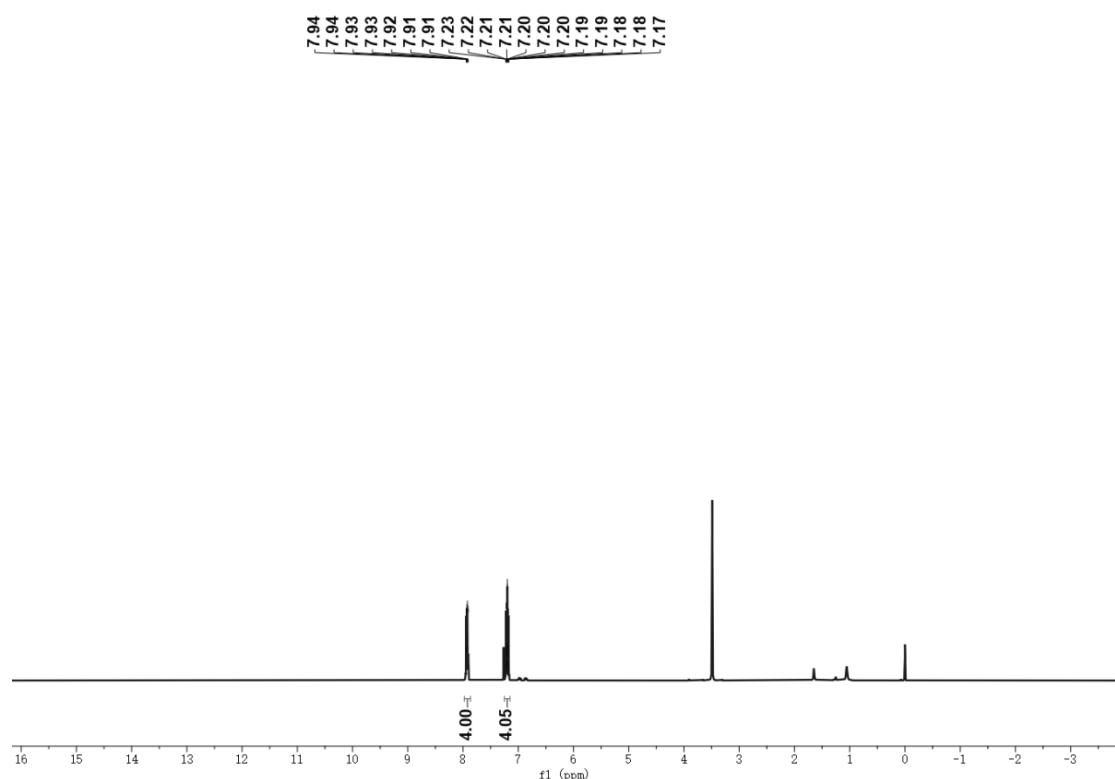


Fig. S24 ^1H NMR spectra of 4,4'-difluoroazobenzene in CDCl_3 .

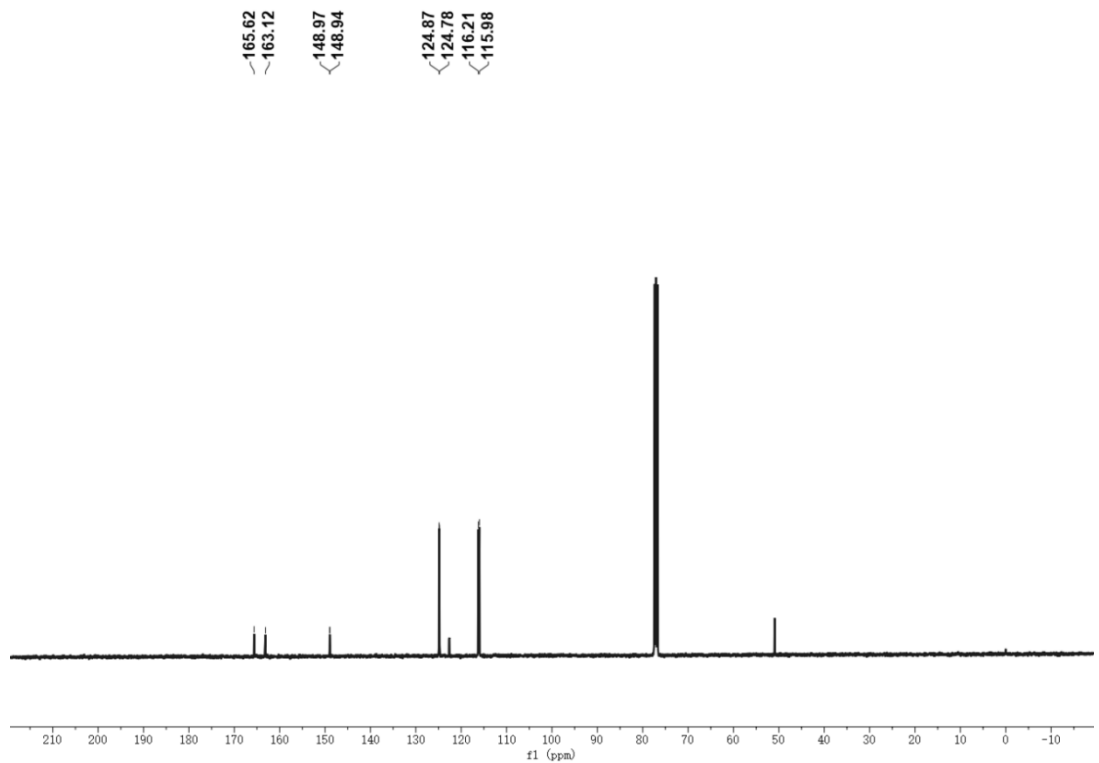
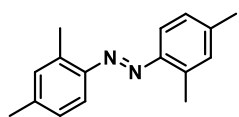


Fig. S25 ^{13}C NMR spectra of 4'4-difluoroazobenzene in CDCl_3

4c. 2,2',4,4'-tetramethylazobenzene



78% yield; ^1H NMR (400 MHz, CDCl_3) δ 7.55 (d, J = 8.2 Hz, 2H), 7.13 (d, J = 1.9 Hz, 2H), 7.05 (dd, J = 8.3, 2.0 Hz, 2H), 2.69 (s, 6H), 2.37 (s, 6H).

^{13}C NMR (101 MHz, CDCl_3) δ 149.19, 140.76, 137.87, 131.80, 127.14, 115.70, 21.41, 17.60.

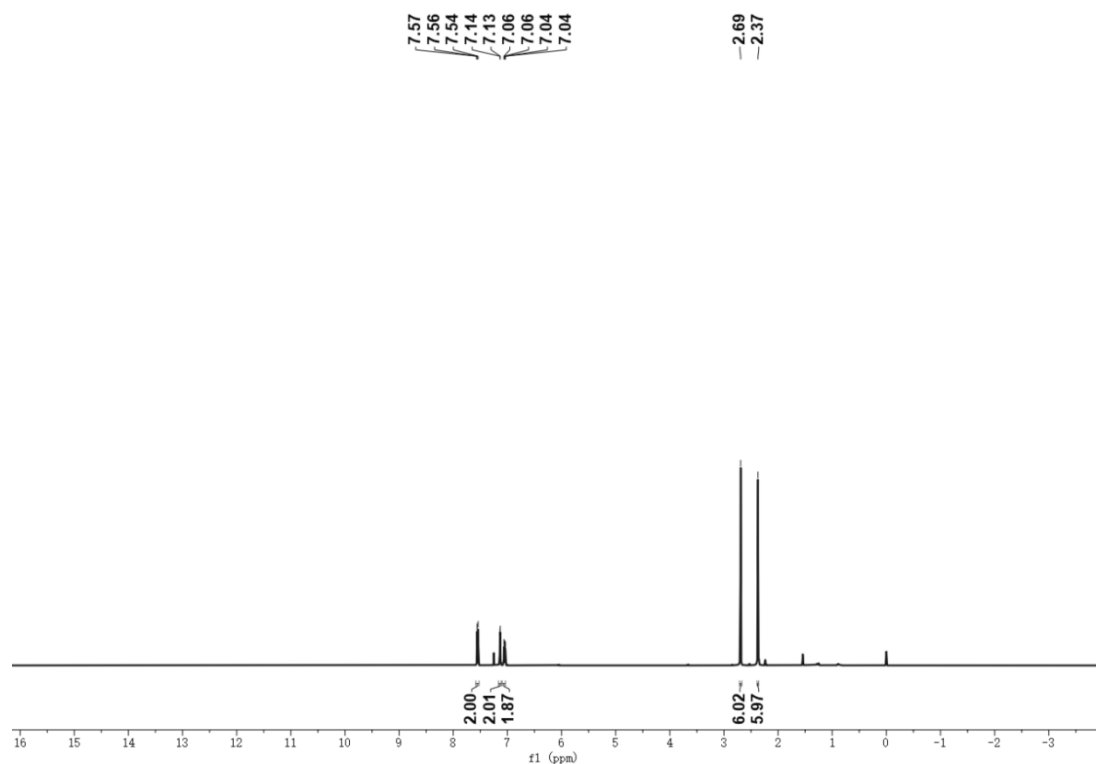


Fig. S26 ^1H NMR spectra of 2,2',4,4'-tetramethylazobenzene in CDCl_3 .

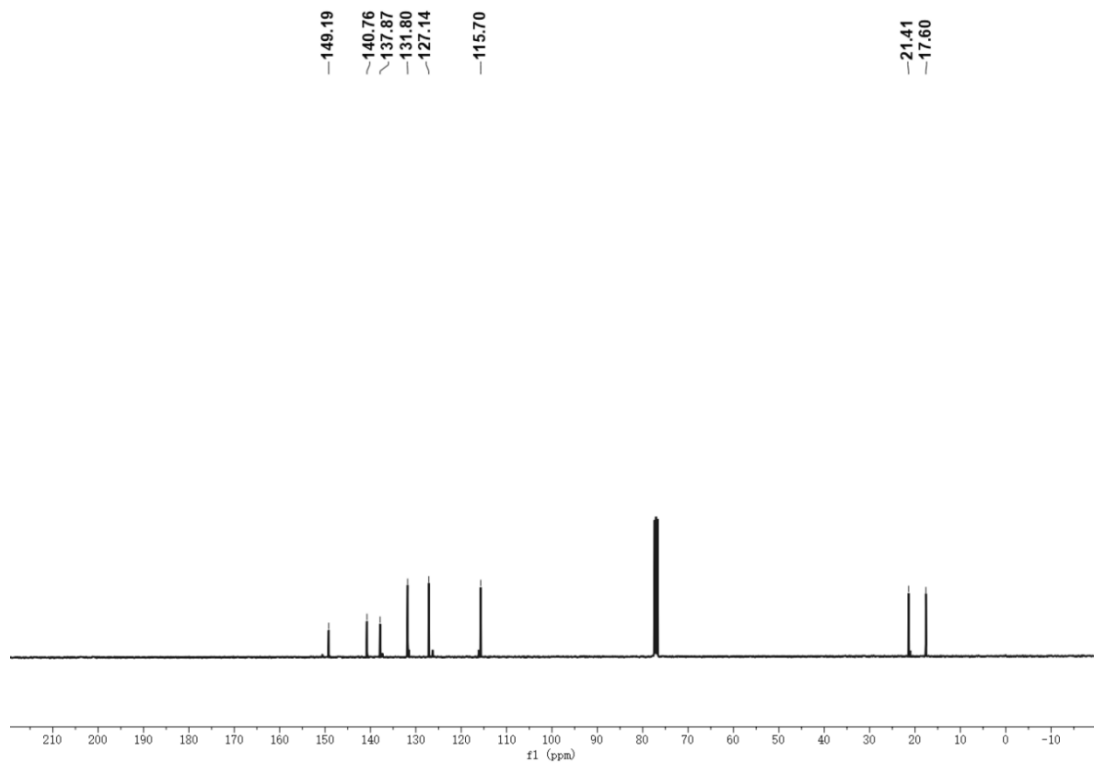
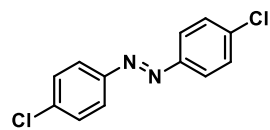


Fig. S27 ^{13}C NMR spectra of 2,2',4,4'-tetramethylazobenzene in CDCl_3 .

4d. 4,4'-dichloroazobenzene



92% yield; ^1H NMR (400 MHz, CDCl_3) δ 7.90 - 7.84 (m, 4H), 7.51 - 7.47 (m, 4H).

^{13}C NMR (101 MHz, CDCl_3) δ 150.77, 137.24, 129.42, 124.21.

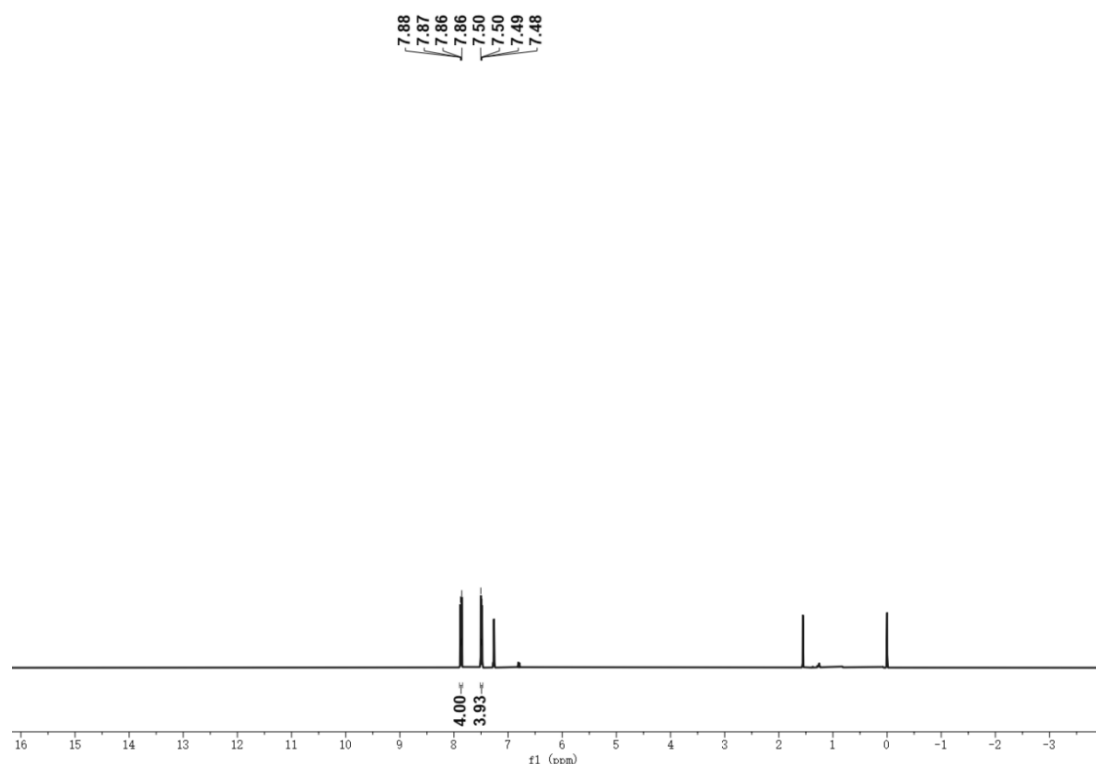


Fig. S28 ^1H NMR spectra of 4,4'-dichloroazobenzene in CDCl_3 .

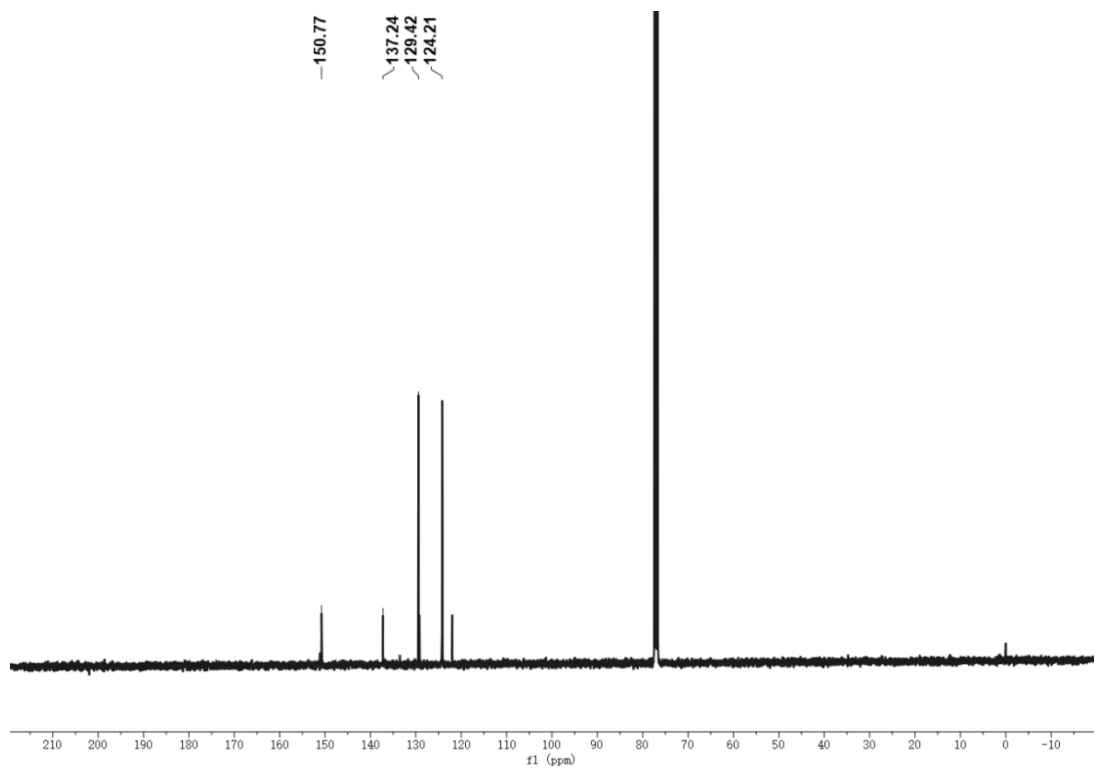
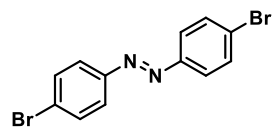


Fig. S29 ^{13}C NMR spectra of 4,4'-dichloroazobenzene in CDCl_3 .

4e. 4,4'-dibromoazo benzene



89% yield; ^1H NMR (400 MHz, CDCl_3) δ 7.82 - 7.78 (m, 4H), 7.67 - 7.63 (m, 4H).

^{13}C NMR (101 MHz, CDCl_3) δ 151.13, 132.42, 125.79, 124.44.

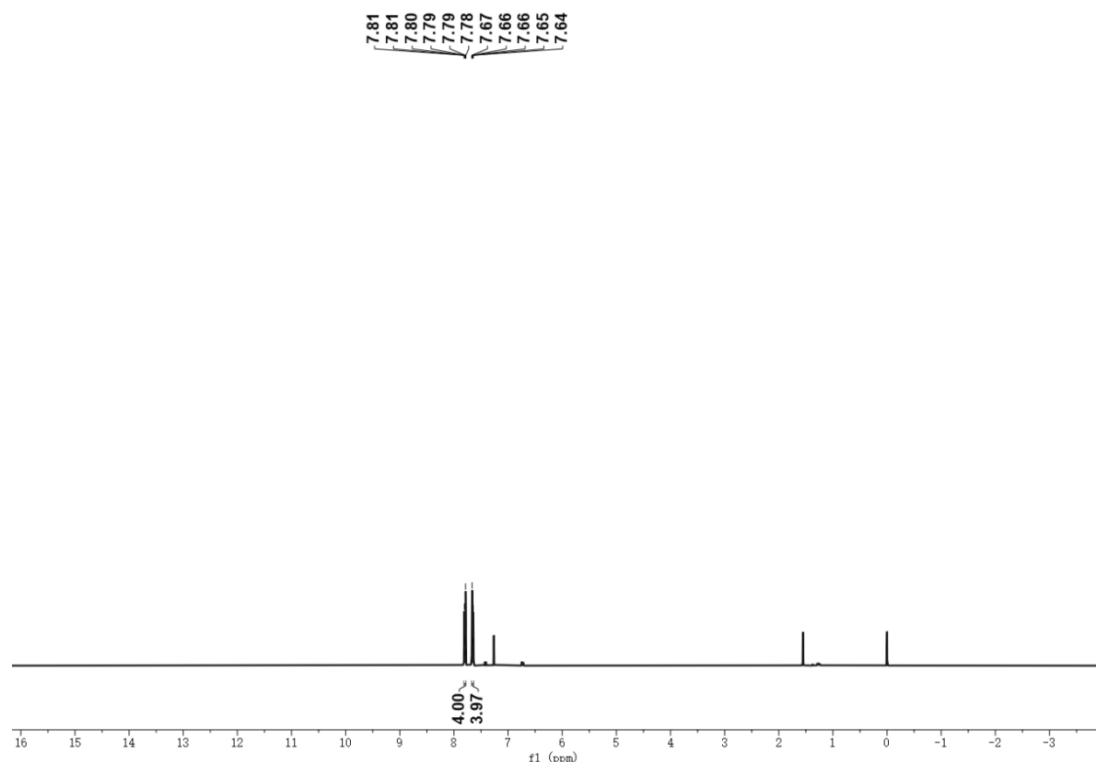


Fig. S30 ^1H NMR spectra of 4,4'-dibromoazo benzene in CDCl_3 .

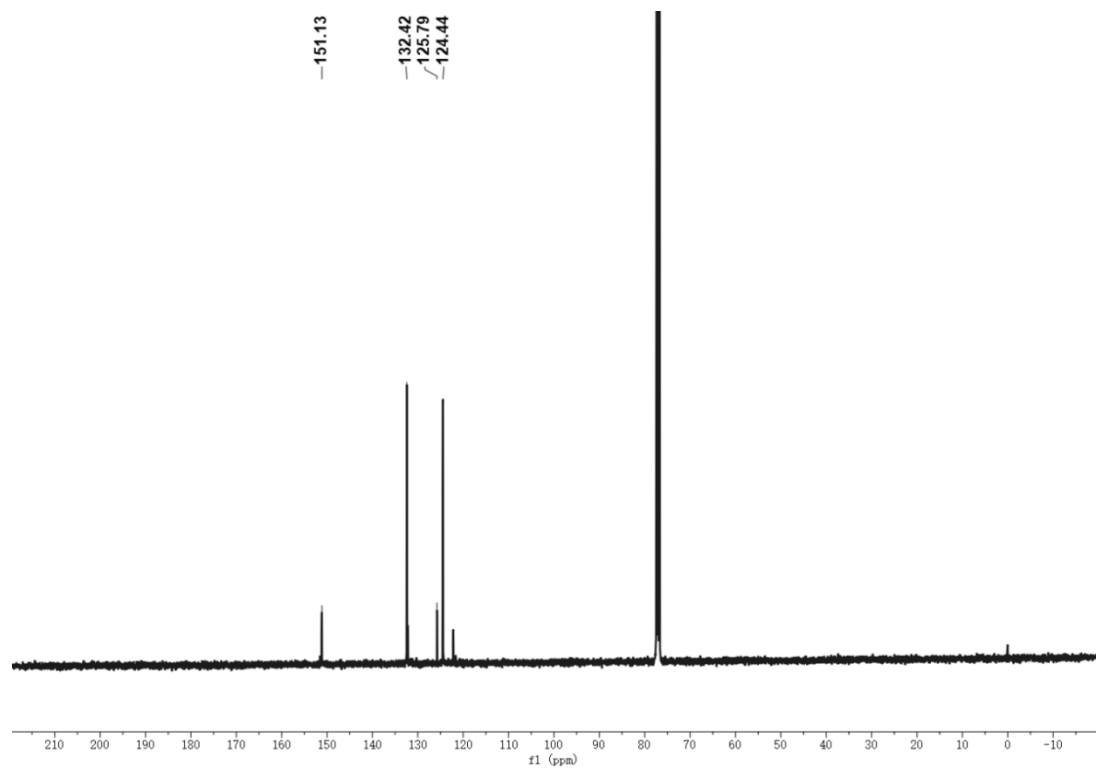
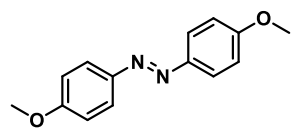


Fig. S31 ^{13}C NMR spectra of 4,4'-dibromoazo benzene in CDCl_3 .

4f. 4,4'-diethoxyazobenzene



86% yield; ^1H NMR (400 MHz, CDCl_3) δ 7.91 - 7.84 (m, 4H), 7.04 - 6.99 (m, 4H), 3.89 (s, 6H).

^{13}C NMR (101 MHz, CDCl_3) δ 161.55, 147.04, 124.35, 114.17, 55.58.

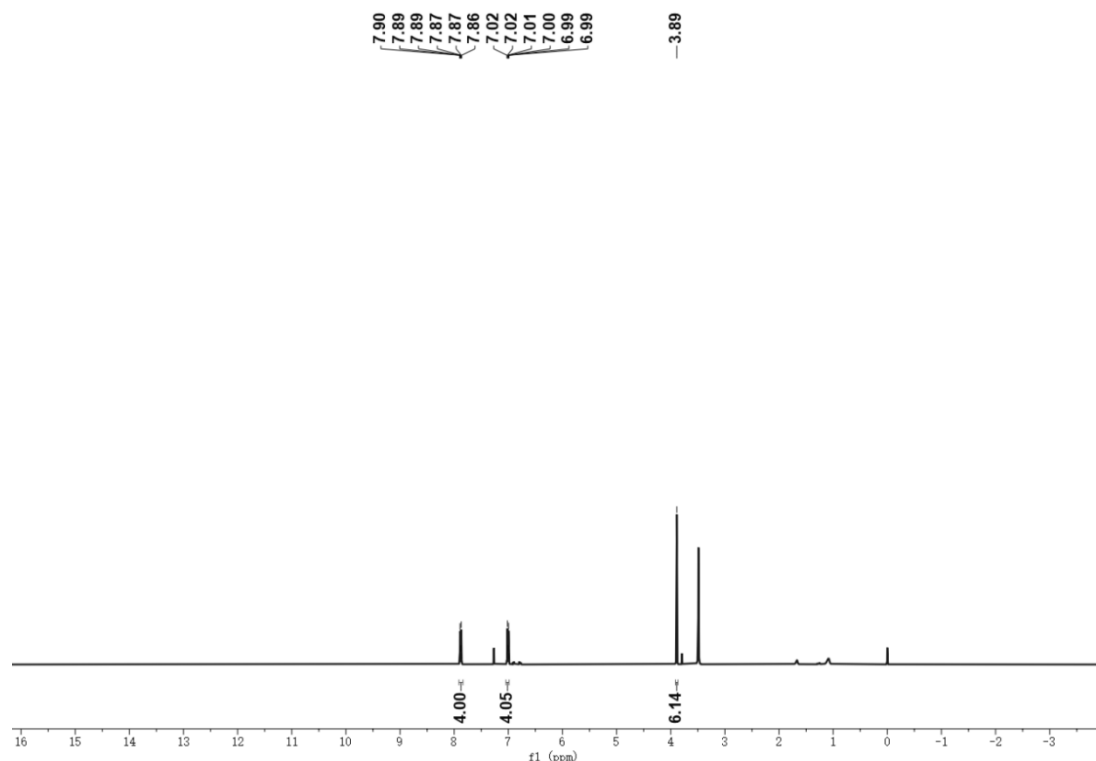


Fig. S32 ^1H NMR spectra of 4,4'-diethoxyazobenzene in CDCl_3 .

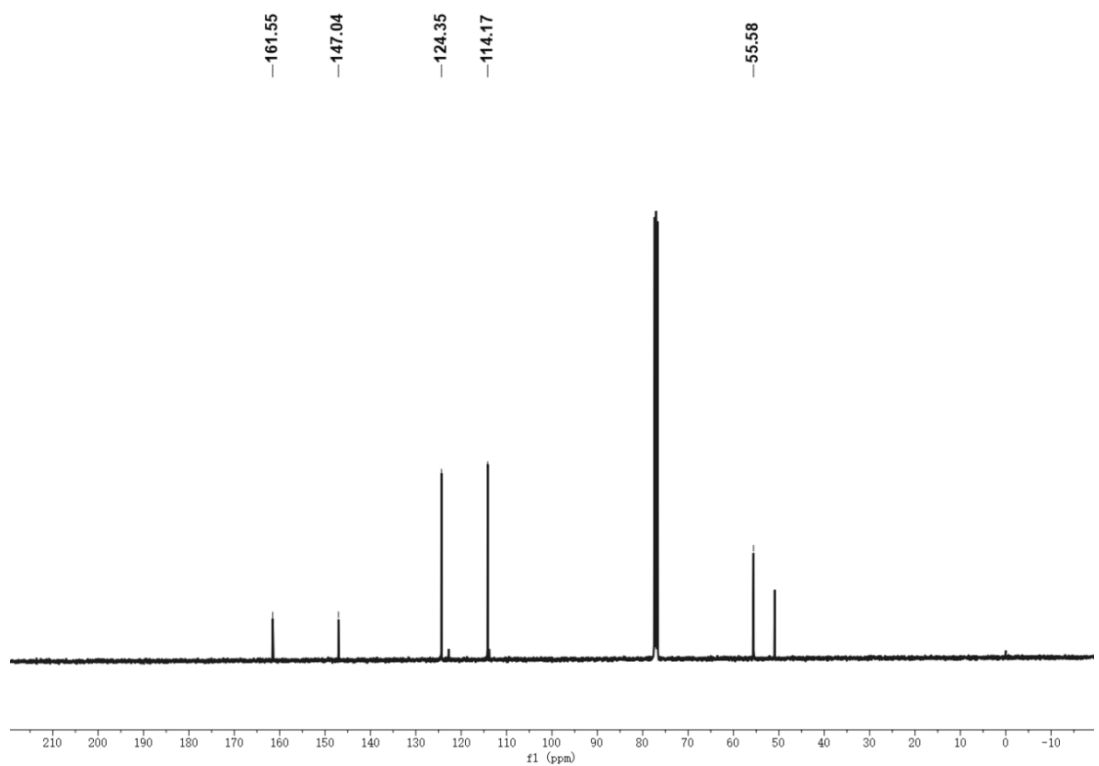
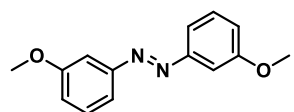


Fig. S33 ^{13}C NMR spectra of 4,4'-diethoxyazobenzene in CDCl_3 .

4g. 3,3'-dimethoxyazobenzene



83% yield; ^1H NMR (400 MHz, CDCl_3) δ 7.60 - 7.54 (m, 2H), 7.50 - 7.39 (m, 4H), 7.04 (ddd, J = 8.2, 2.7, 1.0 Hz, 2H), 3.89 (s, 6H).

^{13}C NMR (101 MHz, CDCl_3) δ 160.32, 153.79, 129.82, 117.92, 117.22, 105.66, 55.51.

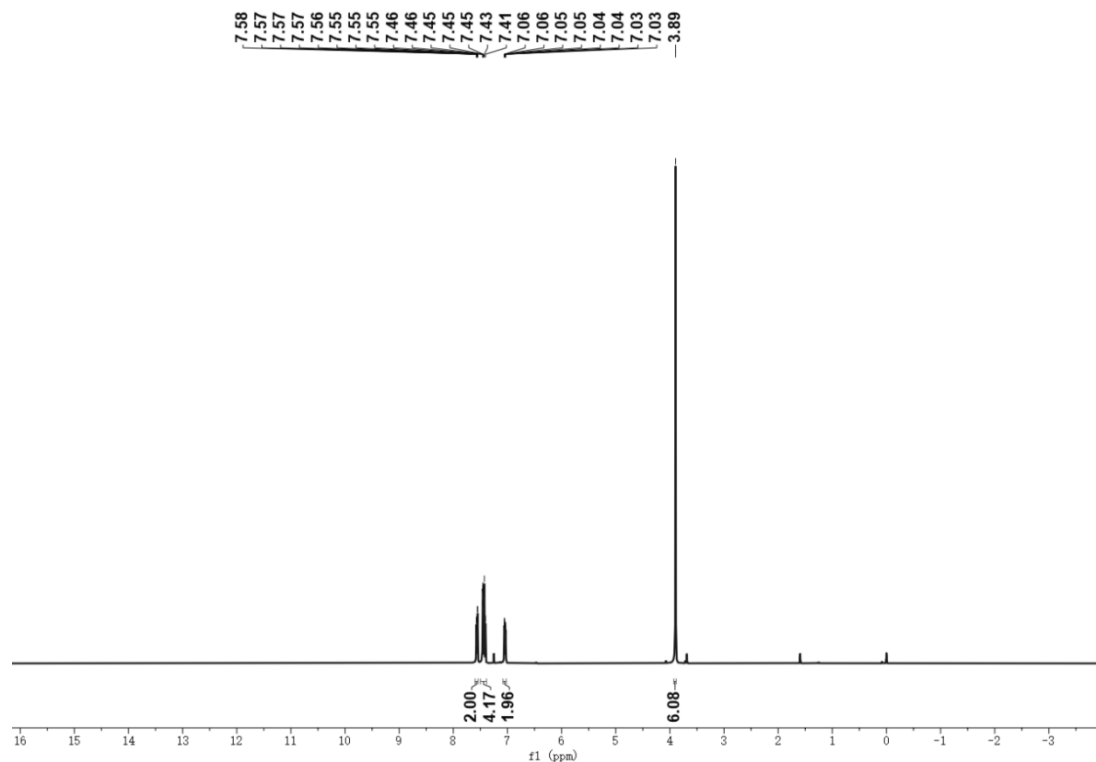


Fig. S34 ^1H NMR spectra of 3,3'-dimethoxyazobenzene in CDCl_3 .

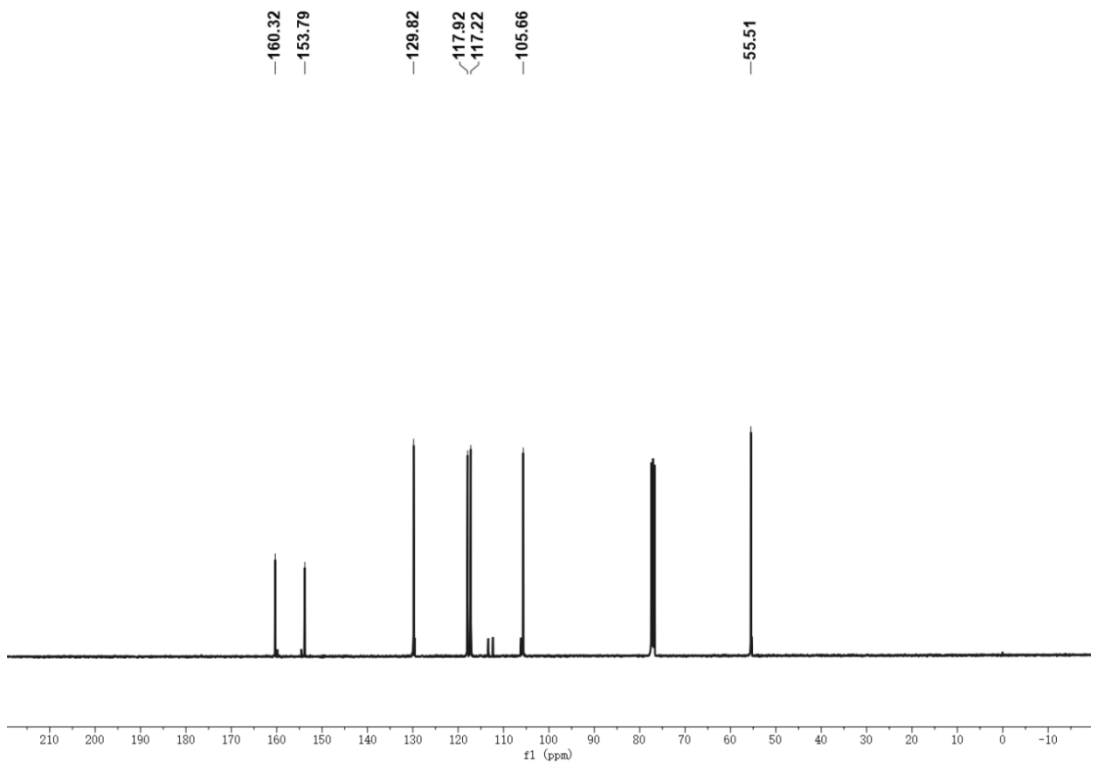
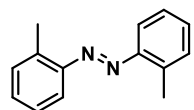


Fig. S35 ^{13}C NMR spectra of 3,3'-dimethoxyazobenzene in CDCl_3

4h. 2,2'-dimethylazobenzene



80% yield; ^1H NMR (400 MHz, CDCl_3) δ 7.67 - 7.57 (m, 2H), 7.38 - 7.31 (m, 4H), 7.25 (ddd, J = 10.3, 5.4, 2.3 Hz, 2H), 2.74 (s, 6H).

^{13}C NMR (101 MHz, CDCl_3) δ 151.08, 138.06, 131.30, 130.73, 126.40, 115.85, 17.67.

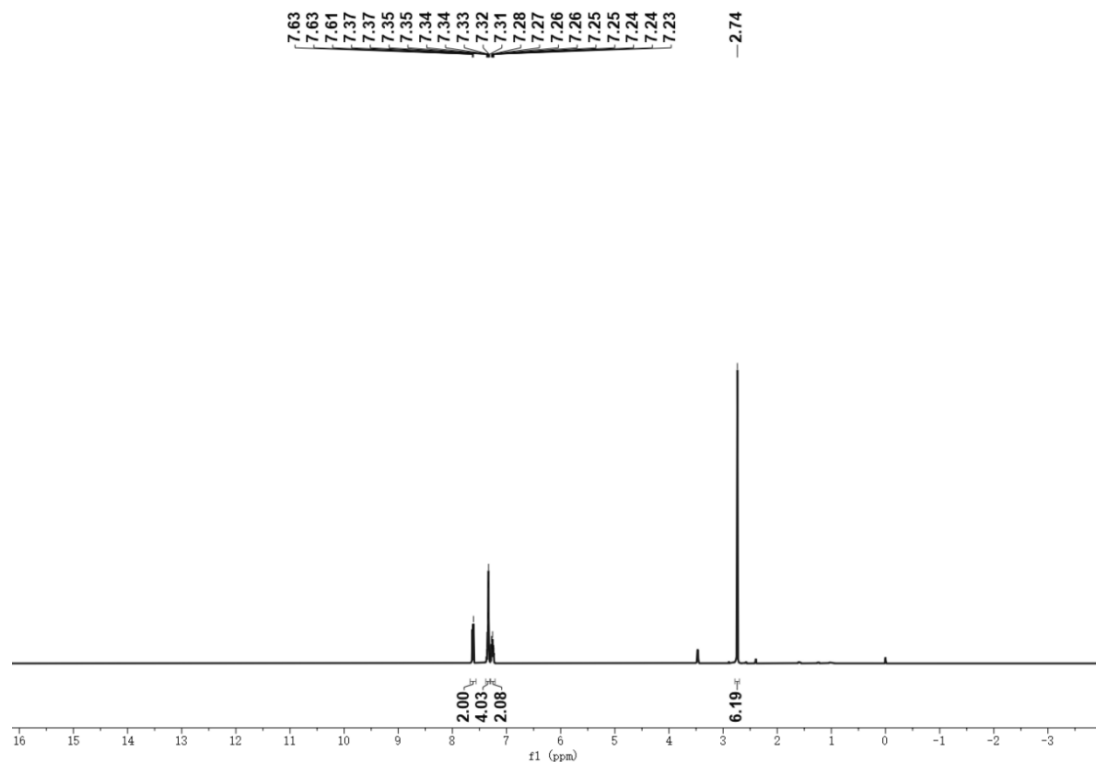


Fig. S36 ^1H NMR spectra of 2,2'-dimethylazobenzene in CDCl_3 .

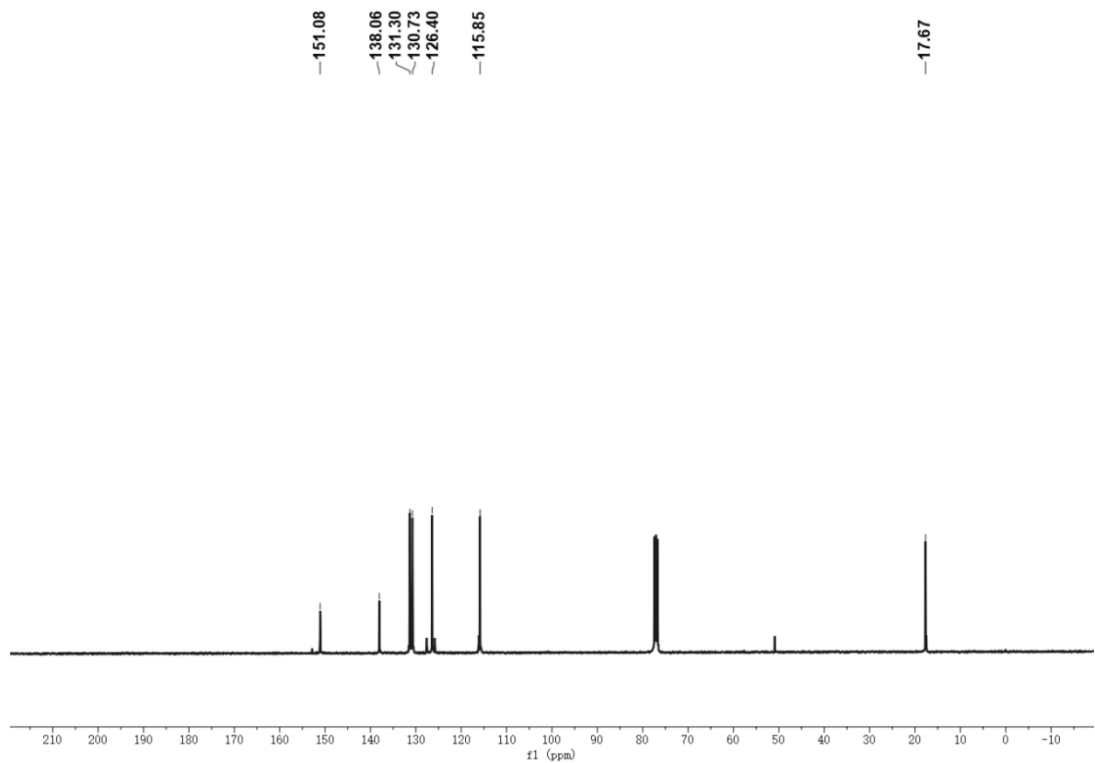
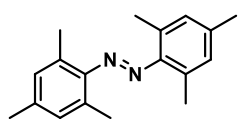


Fig. S37 ^{13}C NMR spectra of 2,2'-dimethylazobenzene in CDCl_3 .

4i. 2,2',4,4',6,6'-hexamethylmethylazobenzene



77% yield; ^1H NMR (400 MHz, CDCl_3) δ 6.96 (s, 4H), 2.41 (s, 12H), 2.34 (s, 6H).

^{13}C NMR (101 MHz, CDCl_3) δ 149.12, 138.38, 131.68, 130.10, 21.09, 20.09.

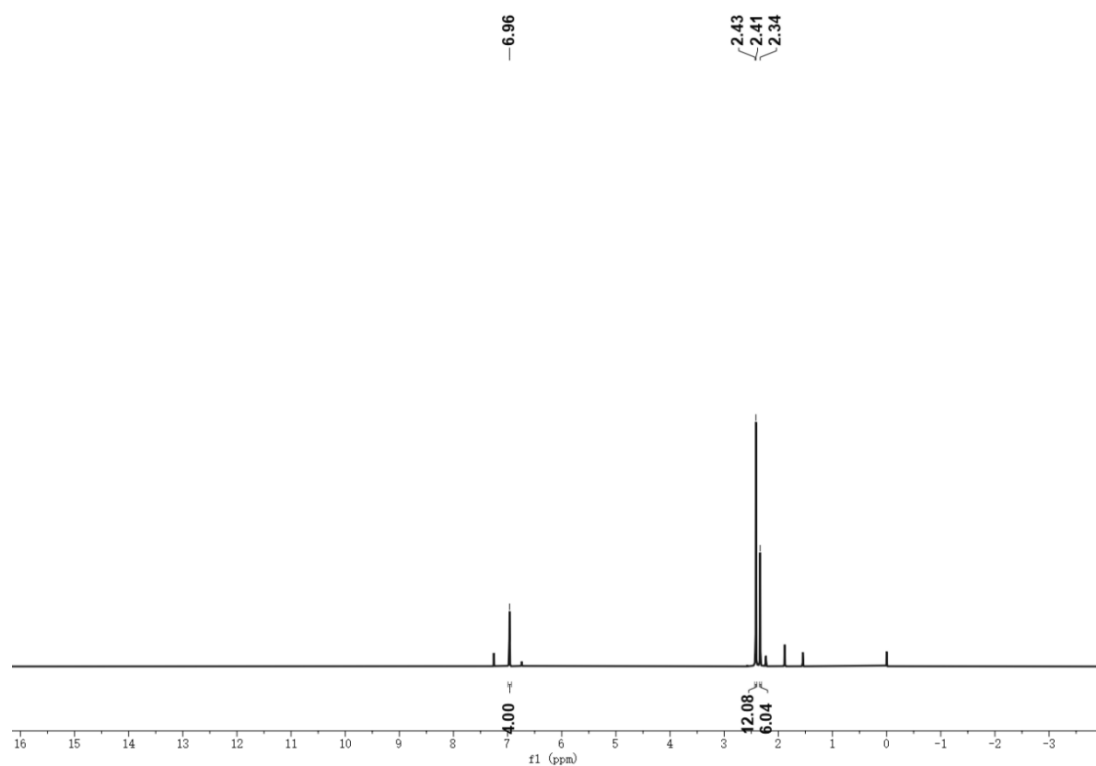


Fig. S38 ^1H NMR spectra of 2,2',4,4',6,6'-hexamethylmethylazobenzene in CDCl_3 .

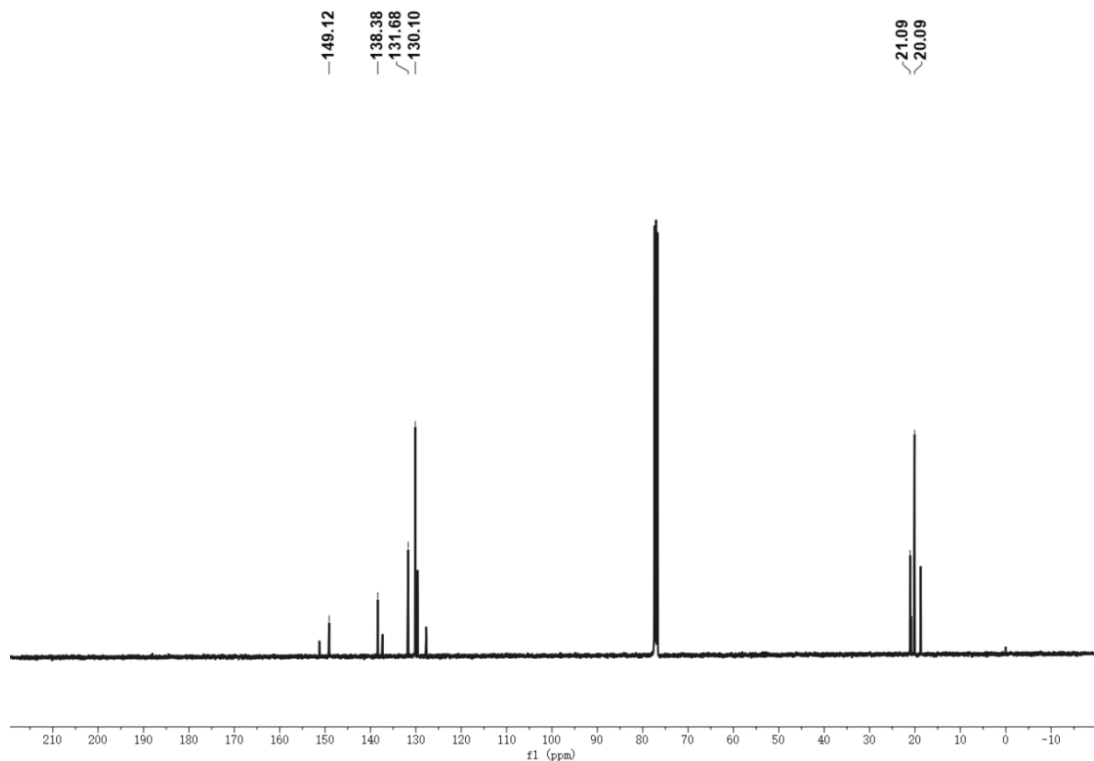
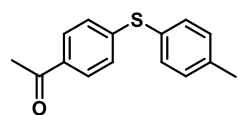


Fig. S39 ^{13}C NMR spectra of 2,2',4,4',6,6'-hexamethylmethylazobenzene in CDCl_3

7a. 4-acetyl-4'-methyldiphenyl sulfide



80% yield; ^1H NMR (400 MHz, CDCl_3) δ 7.82 - 7.75 (m, 2H), 7.45- 7.36 (m, 2H), 7.22 (d, J = 7.8 Hz, 2H), 7.18 - 7.10 (m, 2H), 2.53 (s, 3H), 2.39 (s, 3H).

^{13}C NMR (101 MHz, CDCl_3) δ 145.99, 139.39, 134.55, 130.58, 128.86, 127.87, 126.62, 26.50, 21.33.

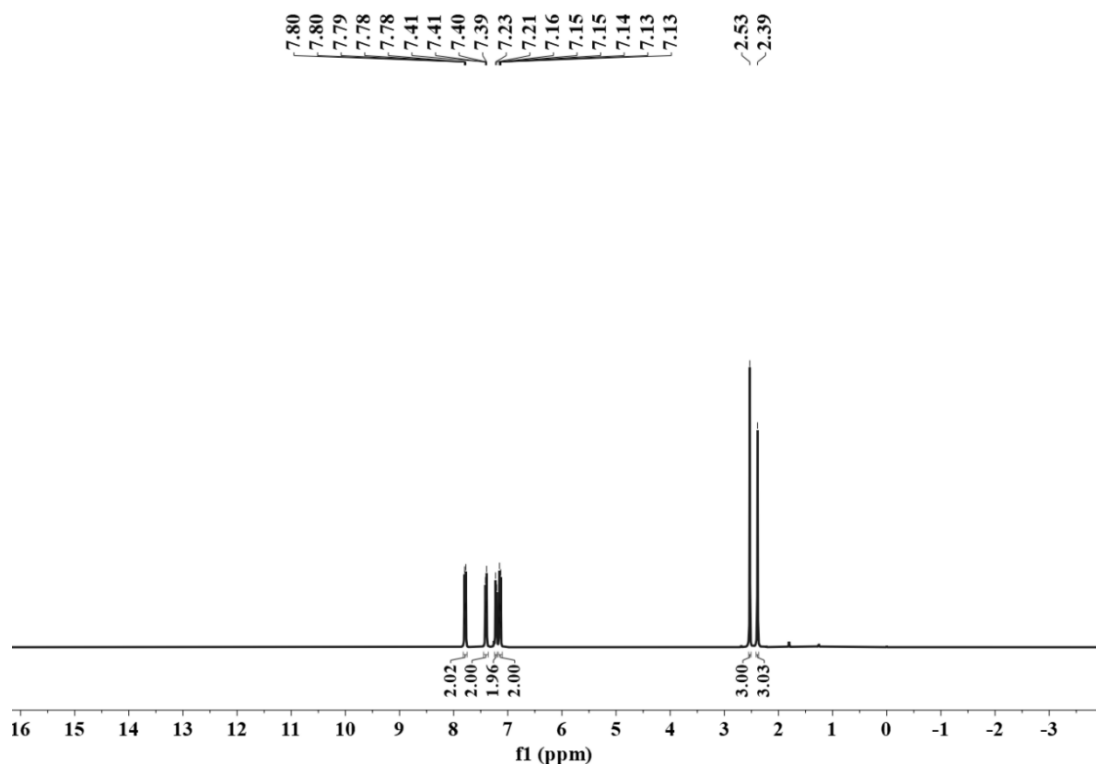


Fig. S40 ^1H NMR spectra of 4-acetyl-4'-methyldiphenyl sulfide in CDCl_3 .

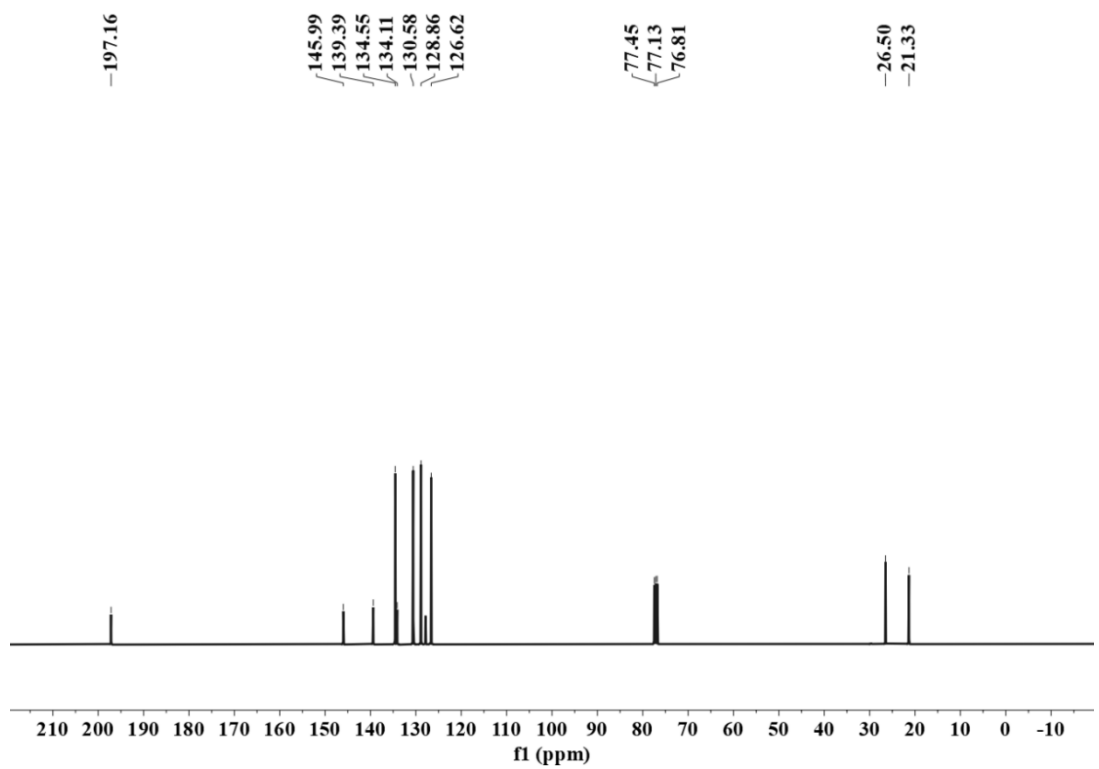
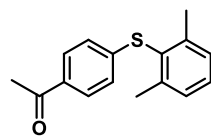


Fig. S41 ^{13}C NMR spectra of 4-acetyl-4'-methyldiphenyl sulfide in CDCl_3 .

7b. 4-acetyl-2,4'-methyldiphenyl sulfide



77% yield; ^1H NMR (400 MHz, CDCl_3) δ 7.76 (d, J = 8.2 Hz, 2H), 7.30 - 7.24 (m, 1H), 7.21 (d, J = 7.5 Hz, 2H), 6.94 (d, J = 8.2 Hz, 2H), 2.52 (s, 3H), 2.40 (s, 6H).

^{13}C NMR (101 MHz, CDCl_3) δ 197.09, 145.35, 144.00, 133.56, 129.93, 128.99, 128.91, 128.73, 124.77, 26.43, 21.75.

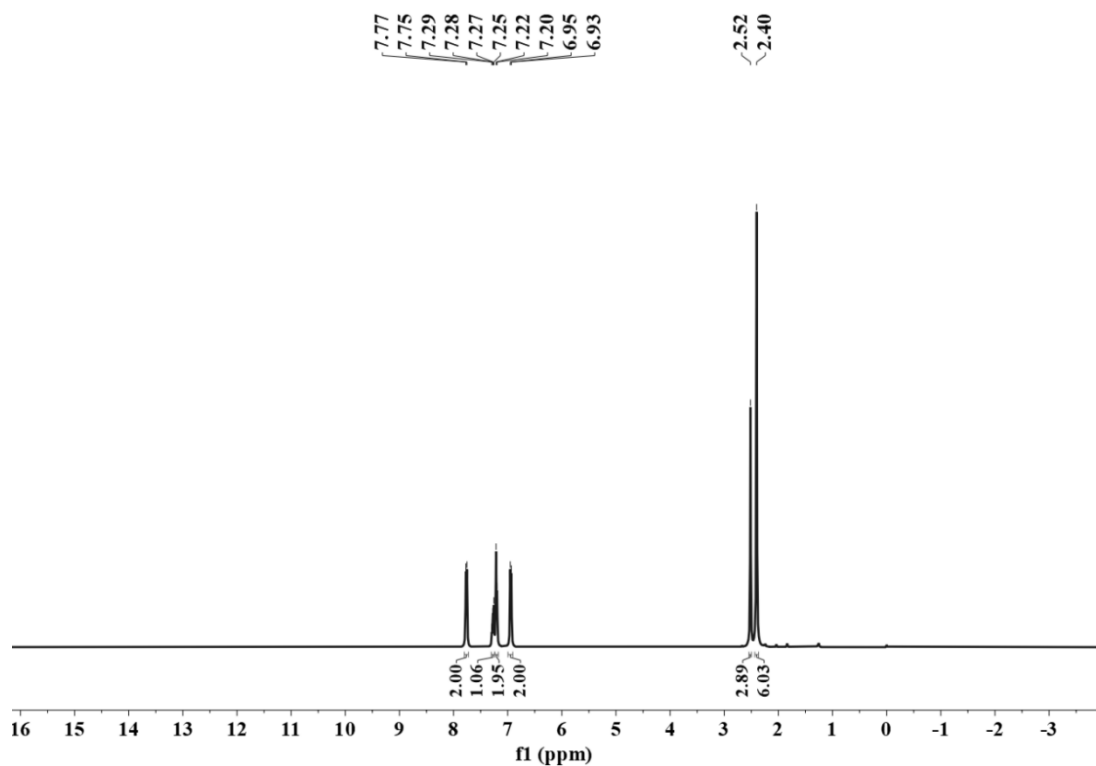


Fig. S42 ^1H NMR spectra of 4-acetyl-2, 4'-methyldiphenyl sulfide in CDCl_3 .

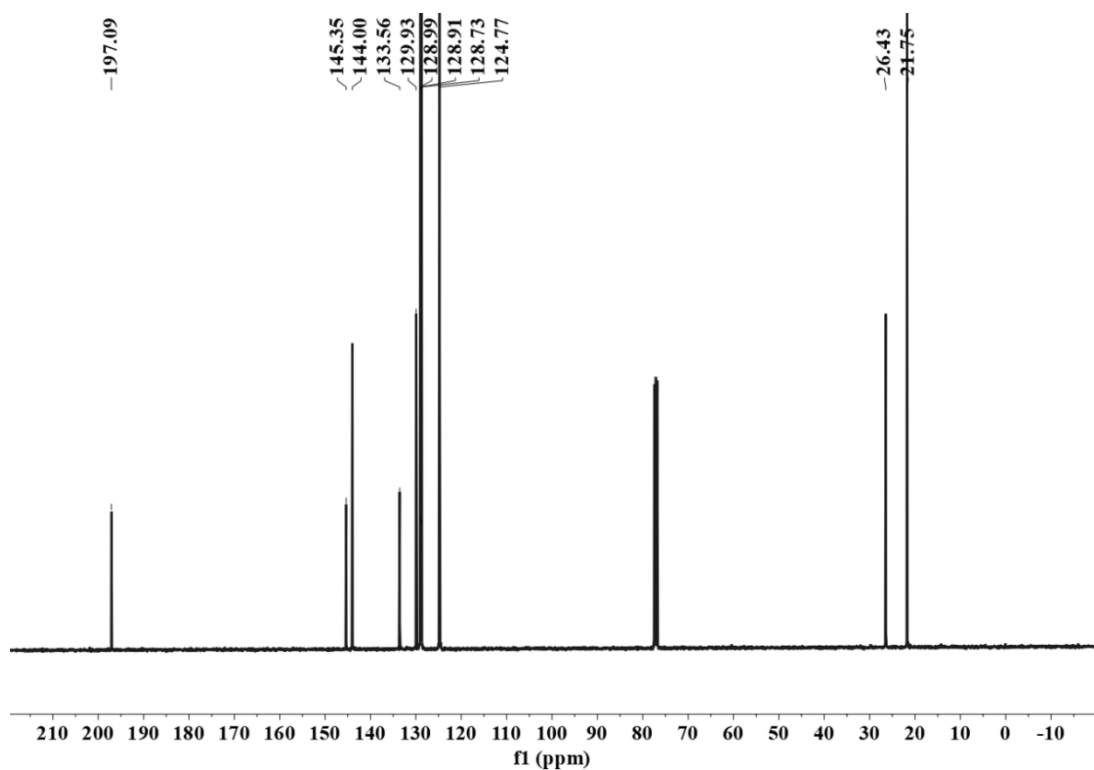
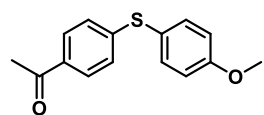


Fig. S43 ^{13}C NMR spectra of 4-acetyl-2, 4'-methyldiphenyl sulfide in CDCl_3 .

7c. 4-acetyl-4'-methoxydiphenyl sulfide



79% yield; ^1H NMR (400 MHz, CDCl_3) δ 7.81 - 7.75 (m, 2H), 7.49 - 7.44 (m, 2H), 7.12 - 7.05 (m, 2H), 6.98 - 6.92 (m, 2H), 3.84 (s, 3H), 2.53 (s, 3H).

^{13}C NMR (101 MHz, CDCl_3) δ 197.16, 160.68, 146.93, 136.87, 133.84, 128.82, 125.77, 121.31, 115.39, 55.44, 26.48.

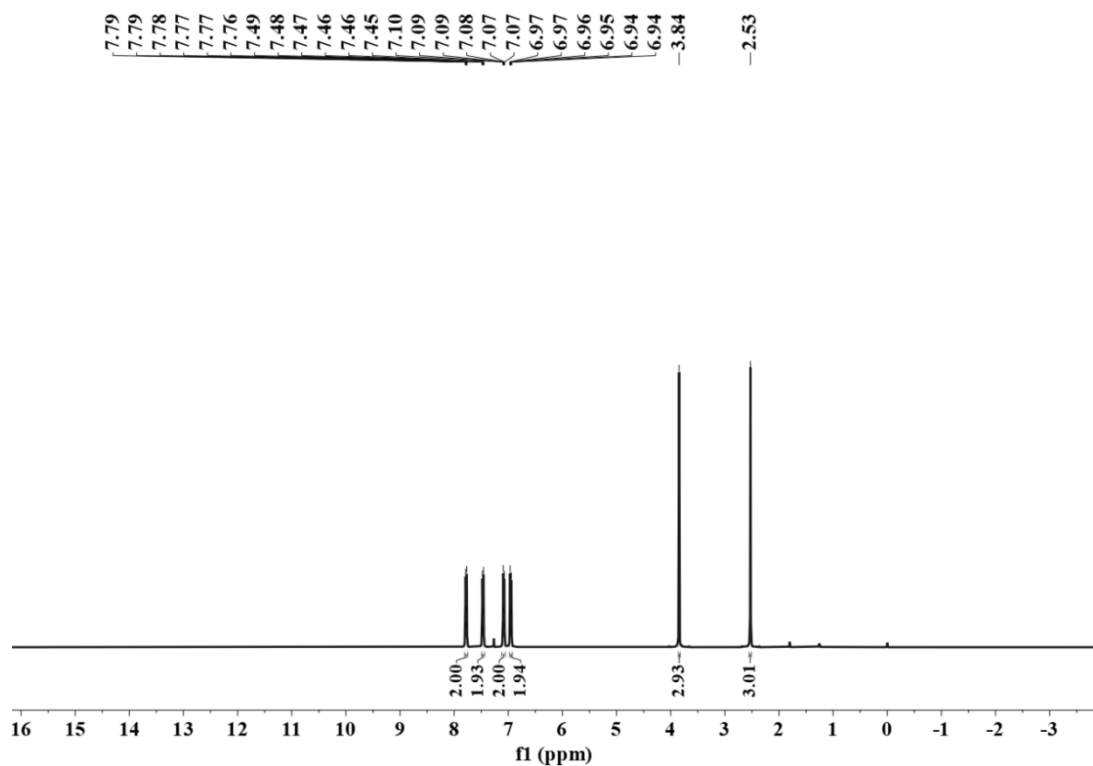


Fig. S44 ^1H NMR spectra of 4-acetyl-4'-methoxydiphenyl sulfide in CDCl_3 .

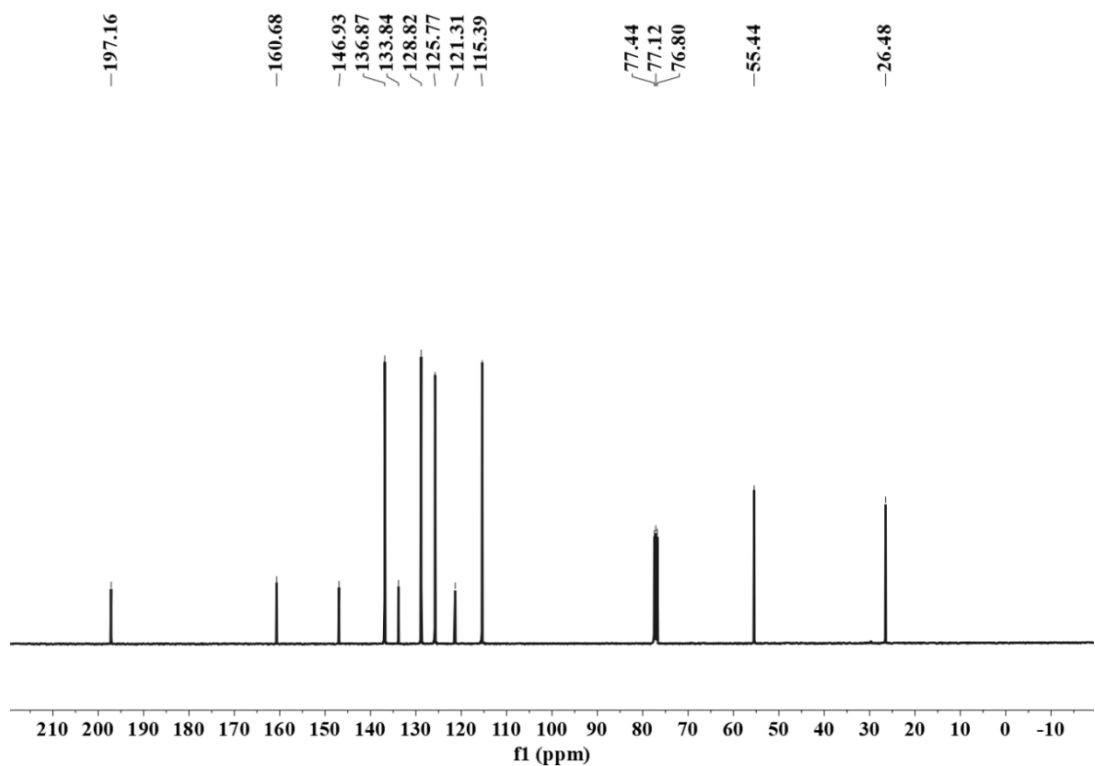
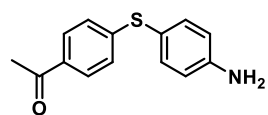


Fig. S45 ^{13}C NMR spectra of 4-acetyl-4'-methoxydiphenyl sulfide in CDCl_3 .

7d. 4-acetyl-4'-aminodiphenyl sulfide



70% yield; ^1H NMR (400 MHz, CDCl_3) δ 7.79 - 7.75 (m, 2H), 7.36 - 7.31 (m, 2H), 7.11 - 7.05 (m, 2H), 6.74 - 6.69 (m, 2H), 3.92 (s, 2H), 2.53 (s, 3H).

^{13}C NMR (101 MHz, CDCl_3) δ 197.29, 147.93, 137.10, 133.57, 128.76, 125.32, 117.58, 116.03, 26.48.

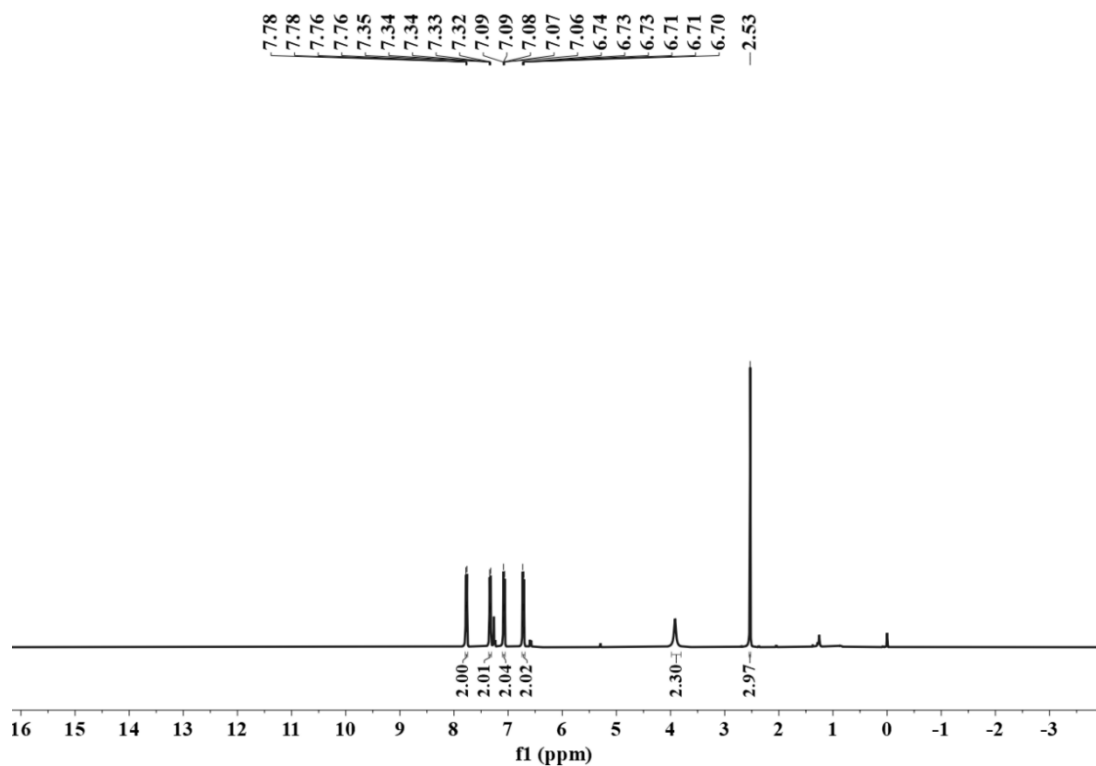


Fig. S46 ^1H NMR spectra of 4-acetyl-4'-aminodiphenyl sulfide in CDCl_3 .

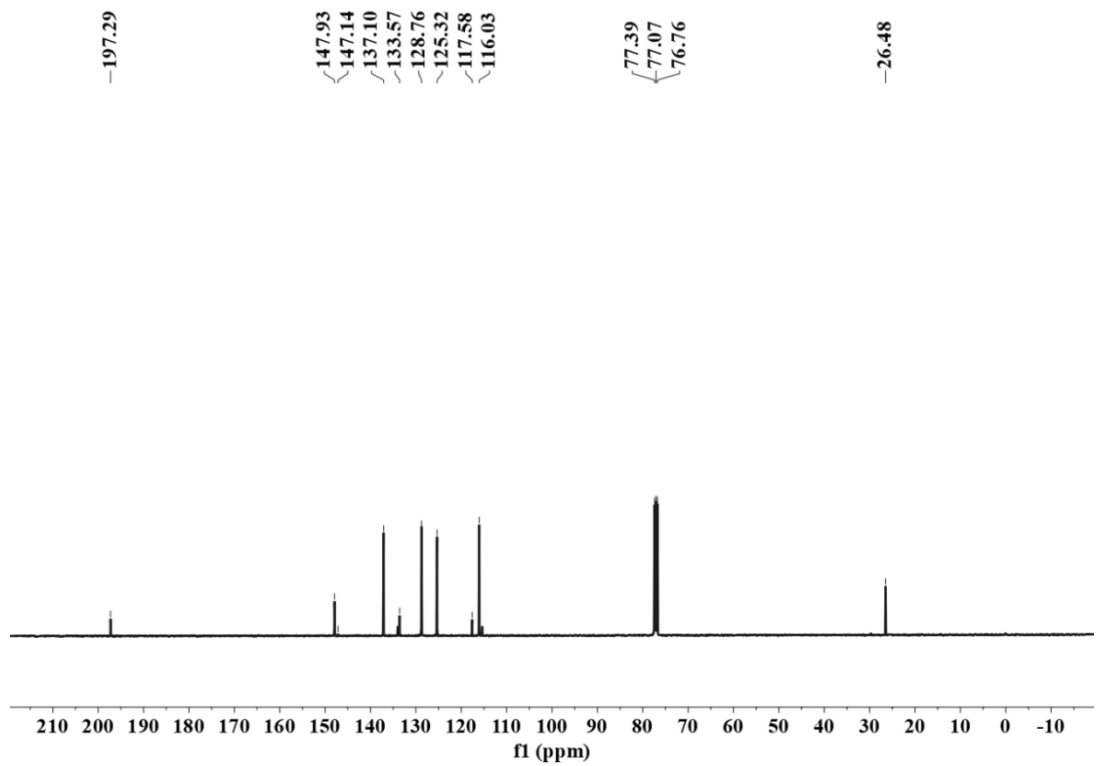
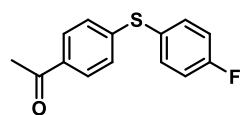


Fig. S47 ^{13}C NMR spectra of 4-acetyl-4'-aminodiphenyl sulfide in CDCl_3 .

7e. 4-acetyl-4'-fluorodiphenyl sulfide



76% yield; ^1H NMR (400 MHz, CDCl_3) δ 7.81 (dq, $J = 8.8, 2.2$ Hz, 2H), 7.54 - 7.44 (m, 2H), 7.17 - 7.05 (m, 4H), 2.54 (s, 3H).

^{13}C NMR (101 MHz, CDCl_3) δ 197.08, 164.51, 162.03, 145.20, 136.61, 136.52, 134.41, 128.96, 126.78, 117.11, 116.89, 26.50.

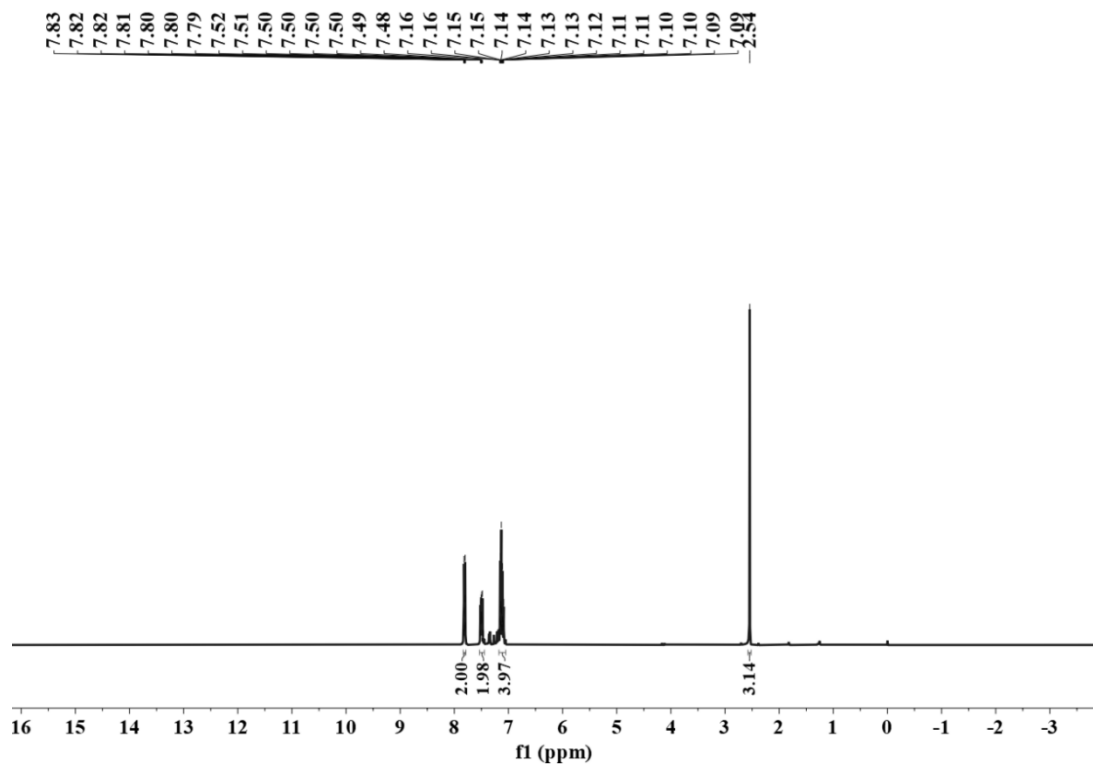


Fig. S48 ^1H NMR spectra of 4-acetyl-4'-fluorodiphenyl sulfide in CDCl_3 .

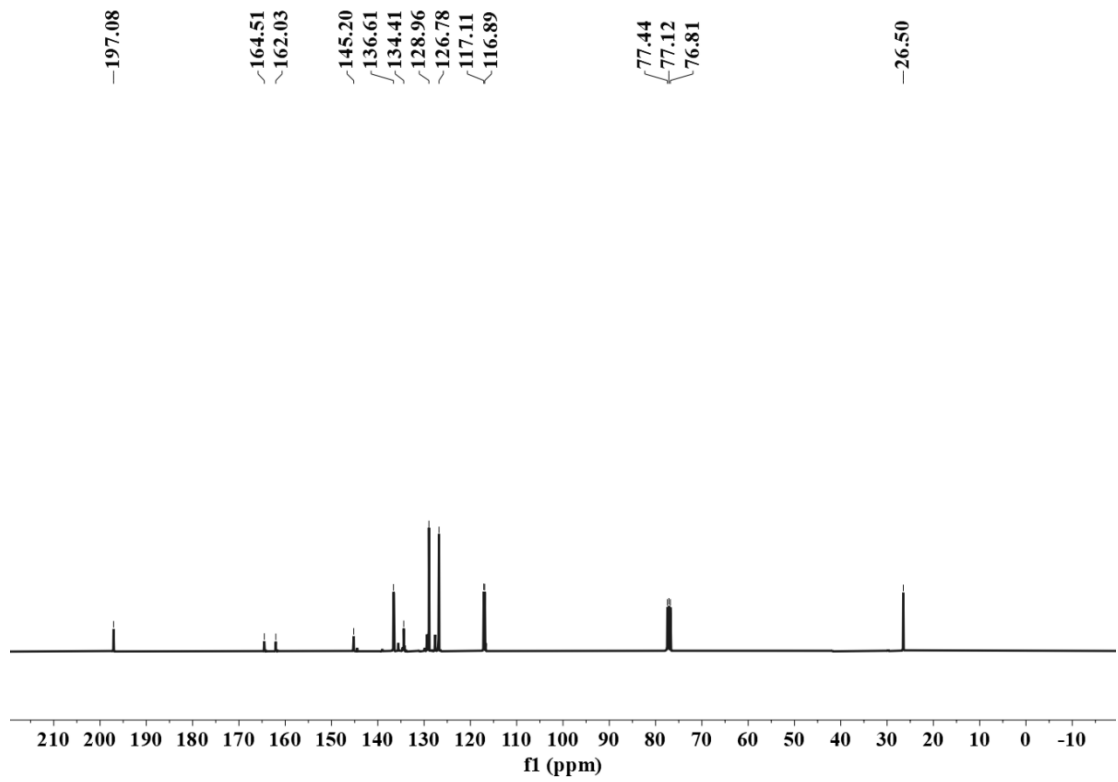
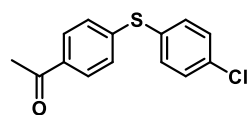


Fig. S49 ^{13}C NMR spectra of 4-acetyl-4'-fluorodiphenyl sulfide in CDCl_3 .

7f. 4-acetyl-4'-chlorodiphenyl sulfide



78% yield; ^1H NMR (400 MHz, CDCl_3) δ 7.86 - 7.81 (m, 2H), 7.44 - 7.34 (m, 4H), 7.24 - 7.19 (m, 2H), 2.56 (s, 3H).

^{13}C NMR (101 MHz, CDCl_3) δ 197.11, 144.06, 134.92, 134.79, 130.89, 129.91, 129.03, 127.78, 26.55.

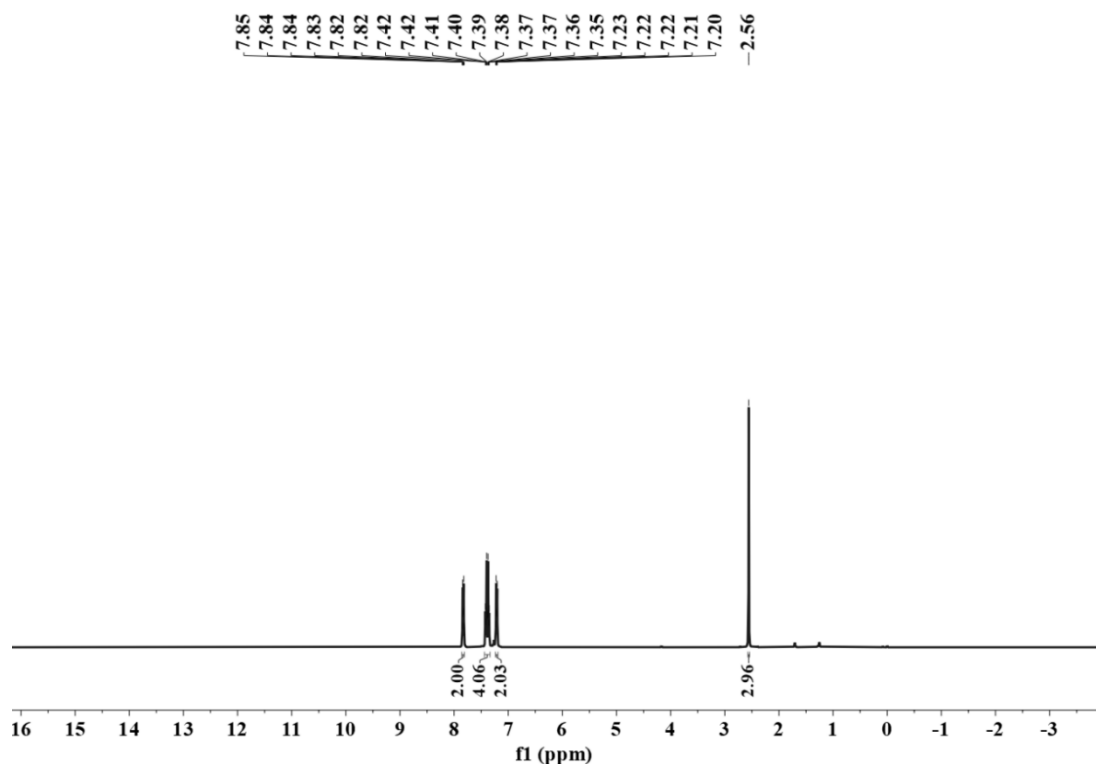


Fig. S50 ^1H NMR spectra of 4-acetyl-4'-chlorodiphenyl sulfide in CDCl_3 .

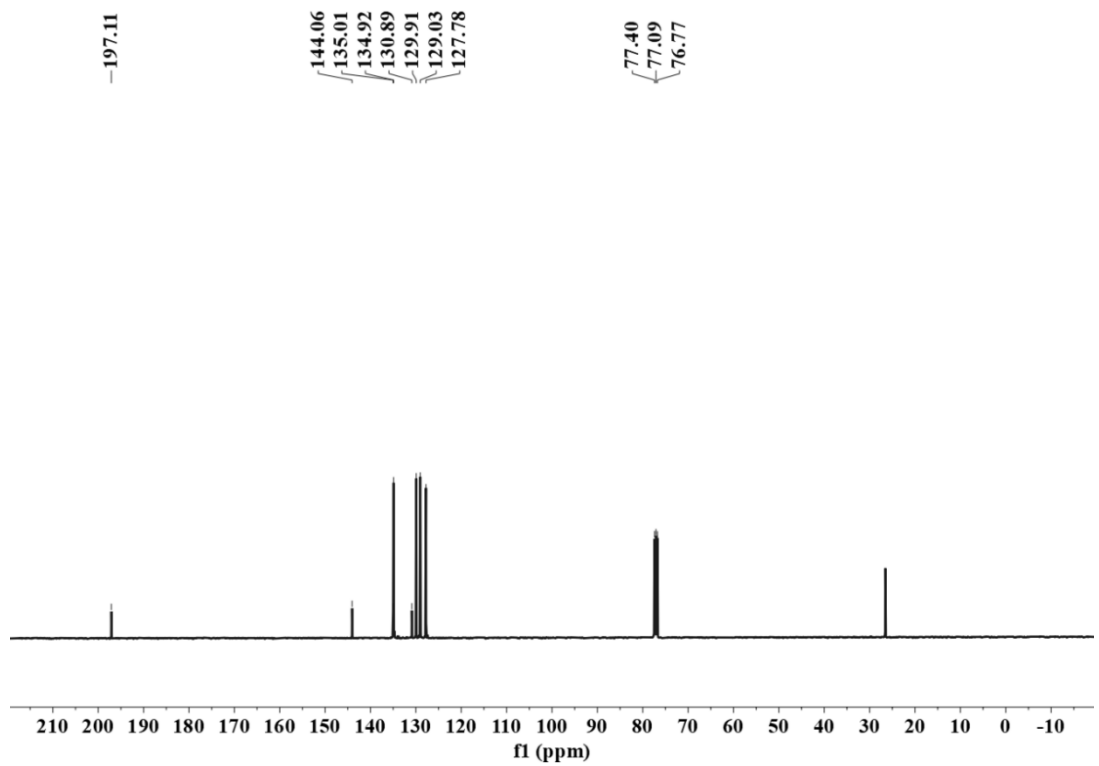


Fig. S51 ^{13}C NMR spectra of 4-acetyl-4'-chlorodiphenyl sulfide in CDCl_3 .